Republic of Iraq

Ministry of Higher Education and Scientific Research

University of Babylon / College of Science

Department of Physics

Study The Nuclear Structure Properties for Some Even-Even Isotones by Using Interacting Boson Model (IBM-1)

A Thesis

Submitted to the Physics Department, College of Science, University of Babylon as a Partial Fulfillment of the Requirements for the Master Degree of in Science in Physics

By

Zahraa Abdul Ameer Kadhum Kshash

B.Sc. in Physics (2019)

Supervised by

Prof.Dr.

Mohammed A. K.Al-Shareefi

Lect.Dr.

Ghaidaa A. Jaber Hussien

2022 A.D. **1444 A.H.**

بسم الله الرحمن الرحيم

﴿ إِنَّ فِي خَلْقِ السَّمَاوَاتِ وَالْأَرْضِ
وَاخْتِلَافِ اللَّيْلِ وَالنَّهَارِ لَآيَاتٍ لِّأُولِي
الْأَلْبَابِ ﴾

صدق الله العلي العظيم

(سورة آل عمران/آية ١٩٠)

Supervisors Certification

We certify that this thesis entitled (**Study The Nuclear Structure Properties for Some Even-Even Isotones by Using Interacting Boson Model (IBM-1)**) was prepared by (**Zahraa Abdul Ameer Kadhum Kshash**) under our supervision at Department of physics, College of Science, University of Babylon, as a partial fulfillment of the requirements for the degree of master of science in physics.

Signature :

Supervisor:

Dr. Mohammed A.K.Al-Shareefi

Title: Professor

Address: Department of Physics College of Science-University of Babylon

Date : / / 2022

Signature :

Supervisor:

Dr. Ghaidaa A.Jaber Hussien

Title: Lecturer

Address: Department of Physics College of Science-University of Babylon.

Date : / / 2022

Certification of the Head of the Department

In view of the available recommendation, I forward this proposal for debate by the examination committee.

Signature:

Name: Dr. Samira Adnan Mahdi

Title: Assistant Professor

Address: Head of the Department of Physics - College of Science - University of Babylon.

Date: / / 2022

Dedication

To whom I proudly bear his name... my dear father

To my angel in life, to the meaning of love and tenderness... my beloved mother

To the best of my life... my brothers

Fahraa

Acknowledgments

First of all, I should thank my Almighty (Allah) for helping me in completing my Thesis.

I would like to express my thanks and gratitude to my supervisors ***Prof. Dr. Mohammed Abdul Ameer Al-Shareefi*** ***and*** ***Lec.Dr. Ghaidaa A. Jaber Hussien*** *for suggesting this topic for me and for their distinguished efforts and sound advice and directions that helped me. In alleviating all the difficulties, I encountered during my work.*

Many thanks are due to the college of sciences at the University of Babylon and the Department of Physics for offering me the opportunity to complete my Thesis.

My great thanks to Prof. Dr. Muhsen Kadhum Mutlab for his kind help and support.

Many thanks and gratefulness to my family who always support me and alleviate difficulties I have faced during my works.

Zahraa

Summary

In this work, the nuclear structure was studied using the interacting bosons model and by applying the IBM program, version 1984 and in the Fortran language.

The Hamiltonian coefficients were estimated for each nucleus and according to their limit, to obtain the best fitting between the theoretical and experimental data available and for the low lying excited energy levels. The electrical transitions between some excited levels, the electric quadrupole moment and the potential energy surface of even-even isotones were also calculated for (^{194}Po, ^{192}Pb, ^{190}Hg, ^{188}Pt,^{186}Os).

As well as determining the shape of the nuclei by studying the potential energy surface using the equations of the potential energy operator, which gives an idea of the deformation that occurs in the nucleus from the deviation of the contour lines and their assembly in a specific area.

The results were compared with the available experimental data, and it was noted that the results showed good agreement. The branching ratios ($R,\ R'\ and\ R''$) were also calculated. The importance of this lies in determining the location of the nucleus relative to the three determinations SU(3), O(6) and U(5), and the results of the current study indicated that the studied nucleus are located within different transitional regions. The results showed that the nucleus ^{194}Po and ^{192}Pb are located in the region U(5), the nucleus ^{190}Hg and ^{188}Pt are in the O(6) region, and the nucleus ^{186}Os is in the O(6)-SU(3) transition region.

Contents

List of Symbols

Symbol	Definition
IBM	The interacting boson model.
IBFM	The interacting boson fermion model.
U(6)	The unitary group.
U(5)	Vibrational Limit.
SU(3)	Rotational Limit.
O(6)	γ-Unstable limit.
N_ρ	Total number of neutron bosons or proton bosons.
N	The neutron number.
PES	Potential energy surface.
β	The deformation parameter.
γ	The angle of deviation from symmetry axes.
$\hat{H}$	The Hamiltonian operator in IBM-1.
$s^\dagger$, $d^\dagger$	The creation operators for *s* and *d* bosons.
$\tilde{s}, \tilde{d}$	The annihilation operators for *s* and *d* bosons.
n_d	The total number of d-boson.
n_s	The total number of s-boson.
eb	Electron barn.
ε	The boson energy.
ε_s	The energy of s- boson.
ε_d	The energy of d- boson.
a_0	The strength of the pairing interacting between the bosons.
a_1	The strength of the angular momentum interacting between the bosons.

Symbol	Definition
a_2	The strength of the quadruple interacting between the bosons.
a_3	The strength of the octupole interacting between the bosons.
a_4	The strength of the hexadecapole interacting between the bosons.
$\hat{P}$	The pairing operator.
$\hat{L}$	The angular momentum operator.
$\hat{Q}$	The quadruple operator.
χ	The quadruple structure parameter.
$\hat{T}_3$	The octoupole operator.
$\hat{T}_4$	The hexadecapole operator.
$\hat{T}^{E_2}$	The electric quadruple operator.
$\hat{T}^{M_1}$	The magnetic dipole operator.
$\hat{T}_m^{(E2)}$	The general multiple E2 operator of the IBM-1.
E2SD =$\alpha_2(e_b)$	The effective charge of s-d boson.
E2DD = β_2	The effective charge of d-d boson.
$\lvert < I_i \lVert \hat{T}^L \rVert I_f > \rvert^2$	the matrix element of (E2) transition.
B(M1)	Reduced magnetic dipole transition probability.
ν	The number of d-boson not paired to zero angular momentum called seniority.
n_Δ	The number of d-boson tripled coupled to zero angular momentum.
L,M	The two quantum numbers which represent the angular momentum and components.

Symbol	Definition
λ, μ	The two quantum numbers which represent the Casmir operator, represent cases SU(3).
K	The number of cases that have equal values of (λ, μ, L).
σ	The number of d-boson not pairwise coupled.
τ	The number of d-boson not pairwise coupled to zero angular momentum.
R, R', R''	The branching ratio.
$E(N, \beta, \gamma)$	The potential energy surface.

List of Figures

List of Tables

CHAPTER ONE

General Introduction

Chapter One

General Introduction

1.1 Introduction

The nucleus is an quantum mechanical system composed of many bodies of protons and neutrons, in which the strong and weak fundamental interactions and electromagnetism play an important role at the most profound level. Therefore the study of the atomic nucleus was crucial to clarifying the origin of matter, which helps to develop a shepe of the nuclear structure, the information contained in the nuclear stability mode, the results of the nuclear reaction, and the spectroscopic analysis of the radiation emitted by the nuclei [1].

Electrostatic interactions and short-range nuclear force of the nucleons in the nucleus play a major role in the stability of the nucleus. This more complex case led to slow progress in developing the acceptable model, and no single nuclear model has been able to describe all nuclear phenomena when protons or neutrons are filled from lower orbitals to higher orbitals to reach specific values such as, 2, 8, 20, 28, 50, 82, 126 [2].

Since the stability of the nucleus is obvious, it takes a large amount of energy to excite the nucleus from one closed shell to another. These numbers are called magic numbers, which manifest as a sudden drop in the observed nucleon separation energies. In alien cores, traditional magic numbers may become invalid, even giving rise to new, previously unrecognized structures [3].

Early in the development of the theory of the nucleus there arose two

very different models. The first model is the nuclear shell model developed by Mayer and Jensen which has its foundation in the single-particle motion of the constituent nucleons in a mean-field potential[4]. The nuclear shell model works well near magic nuclei. However, the model cannot describe features such as rotations and vibrations in nuclei, observed in regions of the nuclear chart distanced from the magic nuclei. The second model is the collective model of Bohr and Mottelson. The collective model is one of the basic models of nuclear structure. Its three main patterns, deformed rotational, spherical vibrational, and γ-soft, continue to be benchmarks to which structure of nuclei are compared [5]

The Interacting Boson Model (IBM) of Arima and Iachello has been successfully applied to a wide range of nuclear collective phenomena. The essential idea is that the low energy collective degrees of freedom in nuclei can be described by proton and neutron bosons with spins of 0 and 2 [6].

The Interacting Boson Model is based on the shell model, which is proved to be a useful tool for studying light nuclei (up to 50 nucleons). The more nucleons there are, the more shells must be considered, and the number of nuclear states quickly grows so huge that the shell model becomes unworkable. The Interacting Boson Model (also known as the Interacting Boson Approximation, or IBA) significantly reduces the number of states. For the 2^+ state indicated above, there are only 26 combinations [7].

1.2 The Nuclear Structure

Nuclear structure physics is useful to the study of the properties of nuclei at low lying excited energy levels, where single energy levels can be resolved. This means that typically quantum effects are predominant

and the states of the nucleus have a very complicated structure that depends on the intricate interrelations of all the many nucleons[8]. The structure of nuclei is more complex than that of atoms. In an atom the nucleus provides a common center of attraction for the electrons, whereas inter electronic forces play a secondary role and the coulomb forces is well understood. In nuclei, there is no center of attraction, the nucleons are held with each others by their mutual interactions[9].

The short range of nuclear forces and the Pauli exclusion principle provide an effective overall force center for each nucleon[9]. The Pauli principle, in its simplest form, embodies the notion that no two identical nucleons can occupy the same place at the same time. More formally, no two nucleons can have identical quantum numbers. In this second form it plays an important role in proton-neutron systems where the two nucleons can be treated as two states of the same nucleon[10].

In nuclear reactions, we study the behavior of nuclei in the relation with other subatomic particles. From a quantum mechanics point view, it is primarily a scattering problem. There are several marked differences from nuclear structure studies[11].

1.3 The Nuclear Models

The presence of amplitudes for many direct product states in a single nuclear eigen state allows the existence of so-called “collective” phenomena, resulting from the addition of these components with coherent phases. Collective structure corresponds semi-classically to coherent motion of nucleons, including possible bulk motion of nuclear matter [12].

The exact nature of the nucleus is still a mystery, many methods have been made towards its understanding. The interaction between nucleons has been studied on the basis of two-body system but the results arrived at can't easily be applied to the many body system. In the absence of any definite and precise theory to account for the complex inter-relationships between nucleons, a number of nuclear models are proposed, each based on a set of simplified assumptions and useful in a limited way [13].

In the following sections, a number of the nuclear models are briefly discussed.

1.4 The Liquid Drop Model

In nuclear physics, the droplet model portrays the nucleus as a drop of incompressible nuclear fluid. George Gamow postulated it originally, then Niels Bohr and John Archibald Wheeler developed it. The fluid is composed of nucleons (protons and neutrons), which are held together by a strong nuclear force. This is a simple model that does not explain all the properties of atomic nuclei, but it does explain the spherical shape of most atomic nuclei. It also helps to predict the binding energy of the nucleus [14].

1.5 The Shell Model

The earliest quantum mechanical model of the nucleus is the nuclear shell model. Its term is derived from the empirical correlation of specific nuclear data. The system is thought to be made up of individual particles traveling in bound orbits in reaction to the rest of the system in a shell

model. Each orbit in which coupling occurs has a specific energy levels, angular momentum, and parity [15].

Many nuclear properties of magic and neighboring nuclei, such as spin, magnetic moment, collective interaction, nuclear parity, quadrupole moment, ground state band , and valence (the valence of the wave function is a property of symmetry under inversion through the origin of the coordinate system, which is a quantity are successfully explained using the shell model. Physical "observable" in quantum mechanics requires that their eigenvalues are real numbers [16]) from even to even nuclei, but fails to explain the properties of other nuclei [13].

1.6 The Collective Model

Because the two models differ in postulates and basic notions, the success of either the shell model or the liquid drop model may lead to major difficulties in developing an inclusive nuclear theory. They also present various explanations for the same nuclear's various nuclear properties. As a result, it's impossible to dismiss the importance of either model. As a result, the two models represent two incomplete pieces of a more comprehensive model that incorporates patterns from both the shell and liquid drop models, resulting in the collective model [17]. Bohr and Mottelson created a unified (collective) model that incorporates some of the features of both the shell and liquid drop models[13]. The nucleons in the nucleus put central press on the nuclear surface, causing the nucleus to be deformed and have a non-spherical shape, according to the collective model. As a result of the liquid drop concept, the surface will vibrate.

The collective attitude nuclei can be deduced from nuclear features such as the initial excited state, where the energy changes significantly as the mass number A grows, with the exception of regions near the closed shell. There are two forms of collective nuclear structures that can be distinguished [18] . To begin with, the nuclear of ($A<150$) exhibits a set of characteristics that may be explained by a model based on vibrations around a balanced spherical form. When the deform nuclei occur at ($150 \leq A \leq 190$), another set of attributes appears, which can be viewed as having a rotating motion for a non-spherical system.

The Bohr and Mottelson collective model was developed from this model to represent quantum mechanical collective motion such as rotations and vibrations [19].

1.7 Isotones and Isotopes

Isotone is an expression used to describe two nuclides if they have the same number of neutrons N but a different number of protons Z (different atomic number) [20].While the isotope refers to the atoms of the same chemical element that have the same atomic number Z, but differ in atomic mass because of the different number of neutrons. The chemical properties of an atom and its counterpart do not differ, because the chemical properties of an atom depend on the number of protons in the nucleus and thus on the number and distribution of electrons orbiting in the nuclear envelope [21]. As the electrons are involved in chemical reactions. As for the physical properties, they differ greatly for both, as they depend on the number of protons and neutrons and their distribution in the nucleus, and they participate in the so-called nuclear reactions[22].

1.8 Literature Survey

We will review the literature study for some authors:

In(2010), **Yue Shi, *et al.* [23]**, studied the potential energy surface of lead, mercury, and polonium isotopes by using IBM-1. The prevalence of high K states is projected to expand the mass region's morphological symbiosis. Where, as in ^{188}Pb, the well-distorted forms give favorable circumstances for the creation of isomers. isomers have been observed systematically in even-even $^{188-196}$Pb and $^{194-210}$Po with the configuration confirmed by g-factor measurements also isomers have also been found experimentally in $^{188-196}$Pb and $^{198-210}$Po . It can be seen that the overall agreement between calculations and data for the observed 11^{-} and 8^{+} isomers in lead isotopes is reasonably good. Also conclude that compared to the situation in lead isotopes, the phenomenon of coexistence between the shape is less well established isotopes of polonium.

In(2011), **K. Nomura, *et al.* [24]**, studied the IBM Hamiltonian's interaction strengths are obtained by mapping the IBM system's potential energy surface (PES). Within the Os and W isotope chains studied, the prolate to oblate phase transition is investigated. When compared to Pt, the nearby isotope, the commencement of this transition is shown to be faster. The calculations also allow for the reduced transition probabilities and excited state energies that are reported for the neutron-rich ^{192,194,196}W nuclei, for which there is only limited experimental data available to date.

In(2012), **Y. Zhang, *et al.* [25]**, studied for the SU(3) limit of the interacting boson model, a unique analytically solvable prolate-oblate

shape phase transitional description is examined in both the finite-N and large-N classical limits. The ground state shape phase transition is proven to be of first order as a result of level crossing. It is demonstrated that this basic innovative description is suitable for describing the prolate-oblate shape phase transition in these nuclei by comparing theoretical expectations with offered experimental data for even even ^{180}Hf, $^{182\text{-}186}$W, $^{188\text{-}190}$Os and $^{192\text{-}198}$Pt, it is shown that this simple novel description is suitable for a description of the prolate-oblate shape phase transition in these nuclei.

In(2013), **F. I. Sharrad, *et al*. [26]**, studied IBM-1 was used to calculate the energy levels, electrical transition probability, B (E2) values, intrinsic quadrupole moment Q_0, and potential energy surface (PES) for ^{184}W and ^{184}Os cores. With intrinsic quadrupole torque, the expected energy levels, transition energy, B (E2) values, and Q_0 results were reasonably consistent with the experimental data. The potential energy surfaces for ^{184}W and ^{184}Os nuclei show that these two nuclei were deformed and have transitional dynamical symmetry SU(3)–O(6) characters.

In(2013), **H. N. Hady and M. K. muttaleb [27]**, studied the symmetry structure of $^{176\text{-}196}$Pt isotopes using the Interacting Boson Model (IBM-1). The energy levels, the electromagnetic transitions probability B(E2), the quadrupole moment of 2_1^+ state and potential energy surfaces are analyzed which reveal the detailed nature of nuclei. In this chain nuclei evolve from harmonic vibrator to gamma soft rotor with wobble a_0/ε ratio ascent and descent in the first four isotopes then steady as straight line in the last six isotopes. The predicted theoretical calculations are compared with the experimental data in respective

figures and tables, it is seen that the predicted results are in a good agreement with the experimental data. In the framework of IBM calculations (40) energy levels were determined for $^{176-196}$Pt isotopes. This investigation increases the theoretical knowledge of all isotopes with respect to energy levels and reduced transition probabilities.

In(2014), **H. H. Kassim and F.I . Sharrad [28]**, studied the isotopes $^{186-198}$Pt, in the O(6) area, with proton number Z = 78 and neutron counts (n) between 108 and 120. The interacting boson model was used to compute the energy level, E2 transition probabilities, rotational energy square, moment of inertia (back bending curve), and potential energy surface in the framework (IBM-1). The estimated results are contrasted to the experimental data that is more unsatisfied. For all of the isotopes, the theoretical and experimental results were in good agreement.

In(2014), **J.E. Garcia-Ramos, *et al.* [29]**, investigated the context of the Interacting Boson Model, including configuration mixing, the evolution of the total energy surface and nuclear shape in the isotope chain $^{172-194}$Pt. When the findings are compared to a self-consistent Hartree-Fock-Bogoliubov computation utilizing the GognyD1S interaction, they show a good agreement. In the region $176 \leq A \leq 186$, the deformation parameters suggests the exist of two alternative coexisting configurations.

In(2015), **J.E. Garcia-Ramos and K. Heyde [30]**, studied used an interactive boson model with formation mixing calculation to investigate the function of gaseous states and the coexistence of pairwise isotopes $^{190-206}$Po. find analyzed the results in the systematics on various observable of the form in Po isotopes behaves in exactly the same way as

in Pt isotopes, that is, it is hidden in some way, in contrast to the situation of Pb and Hg isotopes.

In(2015), **J.E. Garcia Ramos and K. Heyde [31]**, the configuration mixing using Interacting Boson Model, a lengthy chain of polonium isotopes, $^{190\text{-}208}$Po, has been investigated in detail (IBM-CM). fix the Hamiltonians' parameters using a least squares fit to known the levels of energies and electric B(E2) transition rates for states up to 3 Mev excitation energies, electric quadrupole moments, nuclear isotopic shifts and radii, quadrupole shape invariants, wave functions, and deformations were calculated using the IBM-CM Hamiltonians. Virtually all of the examined observables showed good agreement with experimental data, and we conclude that the shape coexistence phenomena is unseen in Po isotopes, just as it is in Pt isotopes.

In(2017), **K.A. Hussain, *et al.* [32]**, studied the low-lying positive parity yrast bands in $^{190\text{-}198}$Hg nuclei were calculated using the Interacting Boson Model (IBM-1). For the O(6) symmetry of these nuclei, the $R_{4/2}$ ratio of the excitation states of the (4_1^+) and (2_1^+) excited states is investigated. Furthermore, we carefully investigated the yrast level $R = E\,L_1^+/E\,2_1^+$ (L= $4_1^+, 6_1^+, 8_1^+, 0_1^+$) of several of the low lying quadrupole collective states in contrast to the existing data as a metric of evolution. We've also looked at the systematic B(E2) values. This calculation's conclusions are in an agreement with the related experimental data. The nuclei are distorted and have γ -unstable-like features, as shown by the contour figures of the potential energy surfaces.

In(2018), **F. Pan, *et al.* [33]**, investigated in order to describe obvious intruder states and nonzero quadrupole moments of γ-soft nuclei such as ^{194}Pt, a rotor extension plus intruder configuration mixing with 2n-particle and 2n-hole configurations from n = 0 up to n → ∞ in the O(6) (γ-unstable) limit of the interacting boson model is proposed. It is shown that the configuration mixing scheme keeps lower part of the γ-unstable spectrum unchanged and generates the intruder states due to the mixing. It is further shown that almost all low-lying levels below 2.17Mev in ^{194}Pt can be well described by modifying the O(6) quadrupole-quadrupole interaction into an exponential form. The third order term needed for a rotor realization in the IBM seems necessary to produce nonzero quadrupole moments with the correct sign

In(2019), **M. M. Hammad, *et al.* [34]**, studied within the framework of the interacting boson model for ^{104}Pd, ^{106}Pd, ^{114}Cd, ^{116}Cd, ^{118}Cd, ^{150}Gd, ^{120}Te, ^{122}Te, ^{118}Xe, ^{120}Xe and q-deformed version of this model, even even near spherical vibrational nuclei with energy ratio $E\,4_1^+/E\,2_1^+$ in the range 2-2.5 are examined utilizing the U(5) dynamical symmetry limit. The parameterization of the U(5) Hamiltonian and its q-deformed counterpart is discovered, resulting in a description of 33 nuclei's energy spectra with a root mean square divergence from experimental level energies of less than 100 keV. The outcomes support the idea that the other dynamic symmetries in the genuine q-deformed vibrational Hamiltonian are quite close.

In(2019), **G. A. Jaber and M. K. Muttaleb [35]**, studied in IBM-1, the energy levels of various mercury isotopes with even - even from 198 to 204 that have gamma unstable features were investigated, and the results were compared to the IBM-2 model. The likelihood of electric

transitions in two models, as well as the ratio of transitions, are included in this paper. Breaking symmetry was investigated in order to fit these isotopes' energy levels and obtain the results from the investigational data. One of the most essential measurements in the study of nucleus structure is the potential energy surface.

In(2021), **J. Kotila [36]**, studied The experimentally measurable observable is the half-life of the decay, which can be factorized to consist of phase space factor, axial vector coupling constant, nuclear matrix element, and function containing physics beyond the standard model. Thus reliable description of nuclear matrix element is of crucial importance in order to extract information governed by the function containing physics beyond the standard model, neutrino mass parameter in particular. Comparison of double beta decay nuclear matrix elements obtained using microscopic interacting boson model (IBM-2) and quasiparticle random phase approximation (QRPA) has revealed close correspondence, even though the assumptions in these two models are rather different. Such comparison is performed using detailed calculations on both models and obtained results are then discussed together with recent experimental results.

In(2021), A. J. Majarshin, *et al.* [37], has been introduced introduce a two-particle, two-hole mixed configuration scheme to fit E2 strengths for the $0_1^+ \rightarrow 2_1^+$, $2_1^+ \rightarrow 4_1^+$, and $4_1^+ \rightarrow 6_1^+$ transitions in ^{194}Pt. The interaction includes two sets of pairing operators, $\{S^{\pm}(t), S^0(t)\}$ (t = s, d). Solutions within this framework are used to analyze energy spectra, E2 transitions, and band-mixing features of the model. The results confirm that mixing is small and similar for J = 2, 4, and 6, with the

calculated energies and transition matrix elements in excellent agreement with experimental data.

1.9 Aim of The Study:

The aim of the current work is to study the nuclear structure of some even-even isotones and to identify their nuclear properties by:

1- Study the low lying of the excited energy levels.
2- Studying the electric transitions probabilities B(E2).
3- Determines the shape of the nuclei by the calculating the potential energy surface.
4- Finding the limit of the isotones as Casten triangle

CHAPTER TWO

Interacting Boson Model (IBM-1)

Chapter Two

Interacting Boson Model (IBM-1)

2.1 Introduction

In 1974 a new model, the interacting boson model, was introduced in an attempt to describe in a unified way collective properties of nuclei. This model is rooted in the spherical shell model developed by Jensen and Mayer, which is the fundamental model for describing properties of nuclei, but in addition has properties similar, and in many cases identical, to the collective model developed by Bohr and Mottelson and based on the concept of shape variables. Since 1974, the interacting boson model has been the subject of many investigations and it has been extended to cover most aspects of nuclear structure[38].

The interacting boson model (IBM) is suitable for describing intermediate and heavy atomic nuclei. Adjusting a small number of parameters, it reproduces the majority of the low-lying states of such nuclei[39].

The interacting boson model deals with nuclei with an even number of protons and neutrons. However, more than half of the nuclear species have an odd number of protons and/or neutrons. In these nuclei there is an interplay between collective (bosonic) and single-particle (fermionic) degrees of freedom. The interacting boson model was extended to cover these situations by introducing the interacting boson-fermion model[40]

The spectroscopy of medium mass and heavy even-even nuclei is characterized by the occurrence of low-lying collective states. The study of nuclear collective motion is one of the most interesting topics in

nuclear physics. The basis for this was laid by Rainwater and Bohr and Mottelson [41].

2.2 Hamiltonian of The IBM-1

The interacting boson model (IBM-1) has been successfully describing collective features of even-even nuclei by using interaction s-bosons and d-bosons [42]. IBM is a six-dimensional Hilbert space characterized by sets of creation and annihilation operators: $s^{\dagger}$, $\tilde{s}$, $d^{\dagger}$, and $\tilde{d}$ [38].

In this model it is assumed that low-lying collective states of even-even nuclei could be described as states of a given (fixed) number N of bosons. Each boson could occupy two levels, one with angular momentum L = 0 (s boson) and another with L = 2 (d boson). In the original form of the model known as IBM-1, proton-boson and neutron-boson degrees of freedom are not distinguished[43].

General forms of IBM-1 Hamiltonian is given by equation (2.1)[44]

$$\widehat{H} = \varepsilon_s\left(s^{\dagger}.\tilde{s}\right) + \varepsilon_d\left(d^{\dagger}.\tilde{d}\right)$$

$$+ \sum_{L=0,2,4} \frac{1}{2}(2L+1)^{\frac{1}{2}} C_L \left[\left[d^{\dagger} \times d^{\dagger}\right]^{(L)} \times \left[\tilde{d} \times \tilde{d}\right]^{(L)}\right]^{(0)}$$

$$+\frac{1}{\sqrt{2}} v_2 \left[\left[d^{\dagger} \times d^{\dagger}\right]^{(2)} \times \left[\tilde{d} \times \tilde{s}\right]^{(2)} + \left[d^{\dagger} \times s^{\dagger}\right]^{(2)} \times \left[\tilde{d} \times \tilde{d}\right]^{(2)}\right]^{(0)}$$

$$+\frac{1}{2} v_0 \left[\left[d^{\dagger} \times d^{\dagger}\right]^{(0)} \times \left[\tilde{s} \times \tilde{s}\right]^{(0)} + \left[s^{\dagger} \times s^{\dagger}\right]^{(0)} \times \left[\tilde{d} \times \tilde{d}\right]^{(0)}\right]^{(0)}$$

$$+\frac{1}{2} u_0 \left[\left[s^{\dagger} \times s^{\dagger}\right]^{(0)} + \left[\tilde{s} \times \tilde{s}\right]^{(0)}\right]^{(0)}$$

$$+ u_2 \left[\left[d^{\dagger} \times s^{\dagger}\right]^{(2)} \times \left[\tilde{d} \times \tilde{s}\right]^{(2)}\right]^{(0)} \qquad (2.1)$$

where $(s^{\dagger},\ \tilde{s})$ and $(\ d^{\dagger},\ \tilde{d})$ are the creation and annihilation operators for (s) and (d) bosons, respectively [45]. This Hamiltonian is specified by nine parameters, two appearing in the one-body terms (ε_s, ε_d) and seven in the two-body terms, [C_L (L = 0,2,4), v_L (L = 0,2), and u_L (L = 0, 2)] [44]. where, (ε_s) and (ε_d) are the single-boson energies and the two-boson interactions had been described by (C_L), (v_L) and (u_L) so on, it shows that for a fixed boson number (N), only one of the one-body term and five of the two body terms are independent, it can be seen, by noting (N = n_s + n_d) [46]. However, it is more common to write the Hamiltonian of the IBM-1 as a multipole expansion, grouped into different boson-boson interactions equation (2.2) [7, 47]

$$\hat{\mathrm{H}} = \varepsilon\, \hat{n}_d + a_0 \hat{P}.\hat{P} + a_1 \hat{L}.\hat{L} + a_2 \hat{Q}.\hat{Q} + a_3 \hat{T}_3.\hat{T}_3 + a_4 \hat{T}_4.\hat{T}_4 \qquad (2.2)$$

where the operators are defined by the following equations:

$\hat{n}_d = [d^{\dagger}.\tilde{d}]$ is operator gives the number of (d) bosons

$\hat{P} = \frac{1}{2}\left(\tilde{d}\ .\ \tilde{d}\right) - \frac{1}{2}\ (\tilde{s}\ .\tilde{s})$ is pairing operator for the (s) and (d) bosons

$\hat{L} = \sqrt{10}\left[d^{\dagger}\ \times\ \tilde{d}\right]^{(1)}$ is the angular momentum operator

$\hat{Q} = \left[d^{\dagger} \times \tilde{s} + s^{\dagger} \times \tilde{d}\right]^{(2)} + \chi\left[d^{\dagger} \times \tilde{d}\right]^{(2)}$ is quadrupole operator

where χ is the quadrupole structural parameter and take the values 0 and ±√7 [38,45].

$\hat{T}_3 = \left[d^{\dagger} \times\ \tilde{d}\right]^{(3)}$ is octupole operators

$\hat{T}_4 = \left[d^{\dagger} \times\ \tilde{d}\right]^{(4)}$ is hexadecapole operators

$\varepsilon = \varepsilon_{\mathrm{d}} - \varepsilon_s$ is the boson energy

ε have ($\Delta n_d = 0$), while ($\hat{P}^{\dagger}.\hat{P}$) has ($\Delta n_d = 0, \pm 2$) and ($\hat{Q}.\hat{Q}$)has ($\Delta n_d = 0, \pm 1, \pm 2$). The strength of the pairing, angular momentum, quadrupole, octoupole, and hexadecapole interaction between the bosons was determined by the parameters, a_0, a_1, a_2, a_3 and a_4 respectively [7].

The IBM Hamiltonian has exact solutions in three dynamical symmetry limits[U(5), SU(3) and O(6)], which are geometrically equivalent to a harmonic vibrator, axial rotor, and γ-unstable rotor respectively.

A form phase transition between the dynamical symmetry limits occurs when the Hamiltonian is represented in terms of an invariant operator of that chain of symmetries [7, 48].

2.3 Electromagnetic Transitions

Electromagnetic transition rates had been characterized by IBM as well, besides agitation energy spectra [49]. The absolute transition rates are not only a sensitive property of nuclear structure, but also provide as a rigorous test for different theories. Coulomb excitation was used to measure the majority of B(E2) values known to date[50].

The general form of the electromagnetic transition rates operators can be written as following [51]:

$$\widehat{T}_m^l = \alpha_2 \delta_{l_2} \left[d^{\dagger} \times \tilde{s} + s^{\dagger} \times \tilde{d}\right]_m^2 + \beta_l \left[d^{\dagger} \times \tilde{d}\right]_m^l + \gamma_0 \delta_{l_0} \delta_{m_0} [s^{\dagger} \times \tilde{s}]_0^0 \quad (2.3)$$

where : l=0,1,2,3,4,…,; m=0,1,2,3,4,…, and $\gamma_{0,}\alpha_2, \beta_l$ represent the specific form of the transition operator, which are parameters specifying the various terms in the corresponding operators[52].

Therefore the electric quadrupole transition operators can be written as [53]

$$\hat{T}_m^{(E2)} = \alpha_2 \left[d^\dagger \tilde{s} + s^\dagger \tilde{d}\right]_m^{(2)} + \beta_2 \left[d^\dagger \tilde{d}\right]_m^{(2)} \quad (2.4)$$

For d- bosons, the magnetic dipole transition operator is given by the formula below[54]:

$$\hat{T}^{(M1)} = \beta_1 \left[d^\dagger \times \tilde{d}\right]_m^{(1)} \quad (2.5)$$

The following expression is the generic formula for the reduced transition probability for electric and magnetic transitions *B(EL),B(ML)* [55].

$$B\left(L, I_i \to I_f\right) = \frac{1}{2I_i + 1} \left| < I_i \| \hat{T}^L \| I_f > \right|^2 \quad (2.6)$$

where $\left| < I_i \| \hat{T}^L \| I_f > \right|$ is the matrix element of (E2) transition.

2.4 Dynamical Symmetries

To solve problems with eigen values in Hamiltonian operators, dynamic symmetries are used [56], Since bosons have six sub- levels in the IBM-1 model where they can be expressed in the form of a unitary group, which is represented by U(6), this can be solved by three dynamical symmetries as follows [57].

2.4.1 Vibrational Limit of The IBM-1 *U*(5)

The dynamic symmetry of the Hamiltonian factor can be calculated using the equation below [58].

$$\hat{H} = \varepsilon \hat{n}_d + a_1 \hat{L}.\hat{L} + a_3 \hat{T}_3.\hat{T}_3 + a_4 \hat{T}_4.\hat{T}_4 \quad (2.7)$$

In this limit, the operators ($\hat{P}$) and($\hat{Q}$) are obviously inefficient, as shown in equation (2.7). The Hamiltonian operator's eigen value equation is given in the formula below [59]:

$$E = \varepsilon_{n_d} + \alpha\frac{1}{2}n_d(n_d-1) + \beta(n_d - v)(n_d + v + 3)$$

$$+\gamma[L(L+1) - 6n_d] \qquad (2.8)$$

The sub-group U(5) and its quantum numbers represent vibrational dynamical symmetry, which can be stated as[60].

$$\left|\begin{matrix} U(6) \supset & U(5) & \supset O(5) & \supset O(3) \supset & O(2) \\ \downarrow & \downarrow & \downarrow & \downarrow & \downarrow \\ [N] & n_d & v, n_\Delta & L & M \end{matrix}\right\rangle \qquad (2.9)$$

where N is the total number of bosons, (n_d) is the number of d-bosons, and (v) is the seniority, which is used to determine the number of d-bosons not pairwise coupled with (L=0). (n_Δ) is the number of tripled d-bosons coupled with (L=0) and (L,M) that are the two quantum numbers to denote the angular momentum and components [54]. Figure (2.1) shows a typical spectrum for the U(5) limit. The following formula is used to calculate the reduced transition probabilities for electric quadruple [61]:

$$B(E2; L+2 \to L) = \frac{\alpha_2^2}{4}(L+2)\big(2N_\rho - L\big) \qquad (2.10)$$

For the ground state

$$B(E2; 2_1^+ \to 0_1^+) = \alpha_2^2\, N_\rho \qquad (2.11)$$

The quadruple momentum can be expressed in the following way [62]:

$$Q_L = \beta_2 \sqrt{\frac{16\pi}{5}} \sqrt{\frac{1}{14}} L \tag{2.12}$$

$$Q_{2_1^+} = \beta_2 \sqrt{\frac{16\pi}{5}} \sqrt{\frac{2}{7}} \qquad For\ 2_1^+\ state \tag{2.13}$$

$$\text{where, } \beta_2 = -\frac{0.7}{\sqrt{2}} \alpha_2 \tag{2.14}$$

The equation below gives the branching ratio R, R' and R'' for U(5) limit [63]:

$$R = \frac{B(E2; 4_1^+ \rightarrow 2_1^+)}{B(E2; 2_1^+ \rightarrow 0_1^+)} = 2\frac{(N_\rho - 1)}{N} \leq 2 \tag{2.15}$$

$$R' = \frac{B(E2; 2_2^+ \rightarrow 2_1^+)}{B(E2; 2_1^+ \rightarrow 0_1^+)} = 2\frac{(N_\rho - 1)}{N} \leq 2 \tag{2.16}$$

$$R'' = \frac{B(E2; 0_2^+ \rightarrow 2_1^+)}{B(E2; 2_1^+ \rightarrow 0_1^+)} = 2\frac{(N_\rho - 1)}{N} \leq 2 \tag{2.17}$$

Figure (2.1) shows an ideal representation of the energy spectrum relying on the quantum number n_d, which is part of the dynamical symmetry U(5).

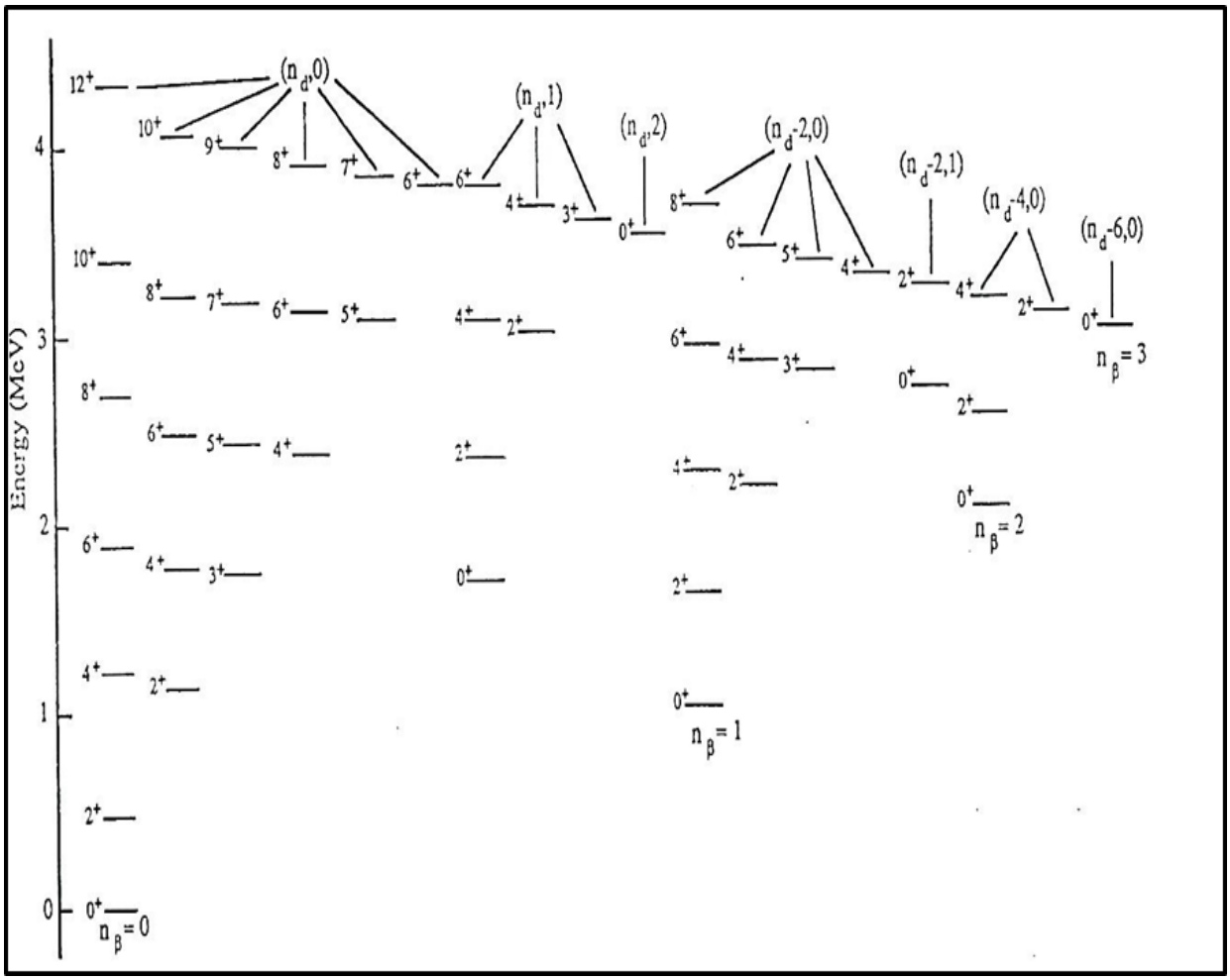

Figure (2.1) A typical spectrum and a quantum numbers for U(5) symmetry [64]

2.4.2 Rotational Limit of The IBM-1 *SU*(3)

The Rotational limit is represented by the sub-group SU(3) [65] where the Hamiltonian for dynamical symmetry can be given in terms of creation and annihilation operators according to the equation below having a_1 and a_2 only[66]:

$$\hat{H} = a_1 \hat{L}\hat{L} + a_2 \hat{Q}\hat{Q} \qquad (2.18)$$

In this limit, the operators ($\varepsilon, \hat{P}, \hat{T}_3$ and $\hat{T}_4$) are ineffectual, as shown by equation (2.18) [67]. The eigen value for this dynamical [68] is:

$$E = \frac{a_2}{2}[\lambda^2 + \mu^2 + \lambda\mu + 3(\lambda + \mu)] + \left(a_1 - \frac{3a_2}{8}\right) L(L+1) \qquad (2.19)$$

Degenerate chain SU(3) can be used to represent the quantum numbers indicated in the eigen value equation [69]

$$\left| \begin{array}{cccc} U(6) \supset & SU(3) \supset & O(3) \supset & O(2) \\ \downarrow & \downarrow & \downarrow & \downarrow \\ [N] & (\lambda, \mu)\mathrm{K} & L & M \end{array} \right\rangle \qquad (2.20)$$

where (K) represents the number of cases with equal values of (λ, μ, L), and the quantum numbers (λ, μ) represent cases SU(3), the equation below shows operator (E2) [70]:

$$T_m^{(E2)} = \alpha_2 \left[\left(d^\dagger \tilde{s} + s^\dagger \tilde{d} \right)_m^{(2)} - \frac{\sqrt{7}}{2} \left(d^\dagger \tilde{d} \right)_m^{(2)} \right] \qquad (2.21)$$

$$\text{where,} \quad \beta_2 = -\frac{\sqrt{7}}{2}\ \alpha_2 \qquad (2.22)$$

The selection rules in this limit are :

$$\Delta\lambda = 0, \Delta\mu = 0$$

The value of *B(E2)* is given by following formula [71]:

$$B(E2; L+2 \to L) = \alpha_2^2\ \frac{3}{4}\ \frac{(L+2)(L+1)}{(2L+3)(2L+5)}$$

$$\left(2N_\rho - L\right)\left(2N_\rho + L + 3\right) \qquad (2.23)$$

For ground state:

$$B(E2\,;2_1^+ \rightarrow 0_1^+) = \alpha_2^2 \frac{1}{5} N_\rho\left(2N_\rho + 3\right) \tag{2.24}$$

For this limit, the electric quadrupole momentum is given [67]:

$$Q_L = -\alpha_2 \sqrt{\frac{16\pi}{40}} \frac{L}{2L+3}(4N+3) \tag{2.25}$$

As $Q_{2_1^+}$ becomes ;

$$Q_{2_1^+} = -\alpha_2 \sqrt{\frac{16\pi}{40}} \frac{2}{7}(4N+3) \tag{2.26}$$

The branching ratios R, R' and R'' for SU(3) limit can be deduced from [38, 54]:

$$R = \frac{B(E2; 4_1^+ \rightarrow 2_1^+)}{B(E2; 2_1^+ \rightarrow 0_1^+)} = \frac{10}{7}\frac{(N_\rho - 1)(2N_\rho + 5)}{N_\rho(2N_\rho + 3)} \leq \frac{10}{7} \tag{2.27}$$

$$R' = \frac{B(E2; 2_2^+ \rightarrow 2_1^+)}{B(E2; 2_1^+ \rightarrow 0_1^+)} = 0 \tag{2.28}$$

$$R'' = \frac{B(E2; 0_2^+ \rightarrow 2_1^+)}{B(E2; 2_1^+ \rightarrow 0_1^+)} = 0 \tag{2.29}$$

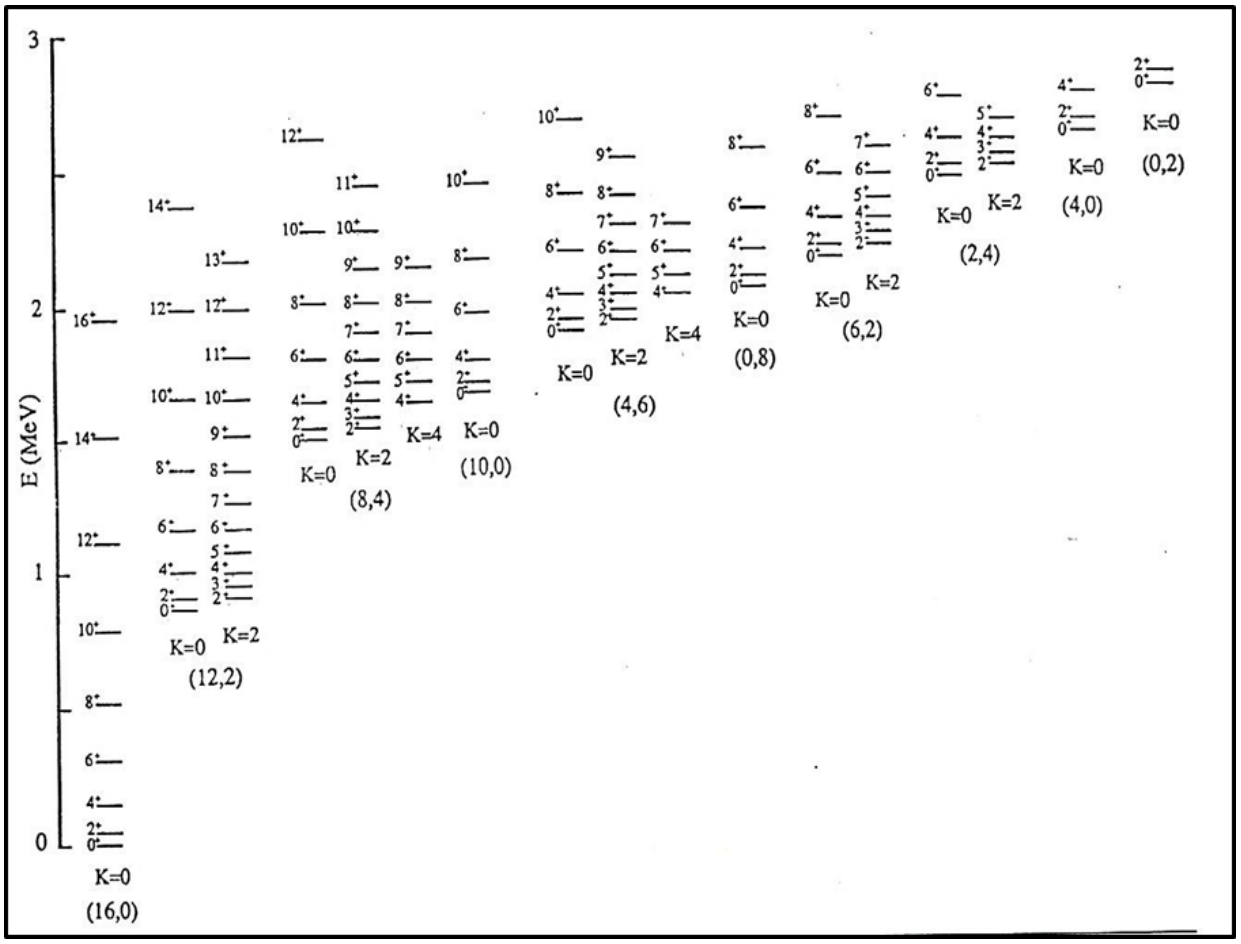

Figure (2.2) A typical spectrum and a quantum numbers for SU(3) symmetry[72]

2.4.3 γ-Unstable Limit of The IBM-1 $O(6)$

This limit is produced when the interaction coupling $(\hat{P}.\hat{P})$ between bosons dominates the energy of bosons (ε) [73]. The Hamiltonian operators in this case is given by[74]:

$$\hat{H} = a_0\hat{P}.\hat{P} + a_1\hat{L}.\hat{L} + a_3\hat{T}_3.\hat{T}_3 \qquad (2.30)$$

The eigen value equation for this dynamical is given [75]:

$$E = A\frac{1}{4}\left(N_\rho - \sigma\right)\left(N_\rho + \sigma + 4\right) + B\frac{1}{6}\tau(\tau+3) + CL(L+1) \qquad (2.31)$$

The quantum numbers for the unstable gamma represented by the sub-group O(6) can be represented by the equation

$$\left| \begin{array}{ccccccc} U(6) & \supset & O(6) & \supset & O(5) & \supset & O(3) \supset O(2) \\ \downarrow & & \downarrow & & \downarrow & & \downarrow \quad \downarrow \\ [N] & & \sigma & & \tau, v_\Delta & & L \quad M \end{array} \right\rangle \tag{2.32}$$

σ, τ: is a quantum numbers which is given as follows:

$\sigma = N_\rho,\ N_\rho - 2, \ldots, 0 \text{ or } 1$, for $\mathrm{N_\rho} = \text{even or odd}$.

$\tau = 0, 1, \ldots, \sigma$.

where ($A = \frac{a_0}{4}$, $B = \frac{a_3}{2}$ and $C = \frac{a_1 - a_3}{10}$) which represent the conjugate eigen value and (v_Δ) represents is number of *d*- bosons tripled coupled with zero angular momentum[75]. Figure (2.3) shows a typical spectrum to O(6) limit[50], the quadrupole transition operator($T_m^{(E2)}$) is [76]:

$$T_m^{(E2)} = \alpha_2 \left[d^\dagger \tilde{s} + s^\dagger \tilde{d} \right]_m^{(2)}. \tag{2.33}$$

where ($\beta_2 = 0$), and the selection rules are ($\Delta\delta = 0, \Delta\tau = \pm 1$), the B(E2) value is given by:

$$B(E2; L+2 \to L) = \alpha_2^2 \frac{(L+2)}{2(L+5)} \frac{1}{4} \left(2N_\rho - L\right)\left(2N_\rho + L + 8\right) \tag{2.34}$$

when L=0 is:

$$B(E2; 2_1^+ \to 0_1^+) = \alpha_2^2 \frac{1}{5} N_\rho \left(N_\rho + 4\right) \tag{2.35}$$

Concludes from the selection rules that the value of quadrupole momentum equals zero: $Q_L = 0$.

The branching ratios R, R' and R'' for the O(6) limit are given by the formulae below[38]:

$$R = \frac{B(E2; 4_1^+ \to 2_1^+)}{B(E2; 2_1^+ \to 0_1^+)} = \frac{10}{7}\frac{(N_\rho - 1)(N_\rho + 5)}{N_\rho(N_\rho + 4)} < \frac{10}{7} \qquad (2.36)$$

$$R' = \frac{B(E2; 2_2^+ \to 2_1^+)}{B(E2; 2_1^+ \to 0_1^+)} = \frac{10}{7}\frac{(N_\rho - 1)(N_\rho + 5)}{N_\rho(N_\rho + 4)} < \frac{10}{7} \qquad (2.37)$$

$$R'' = \frac{B(E2; 0_2^+ \to 2_1^+)}{B(E2; 2_1^+ \to 0_1^+)} = 0 \qquad (2.38)$$

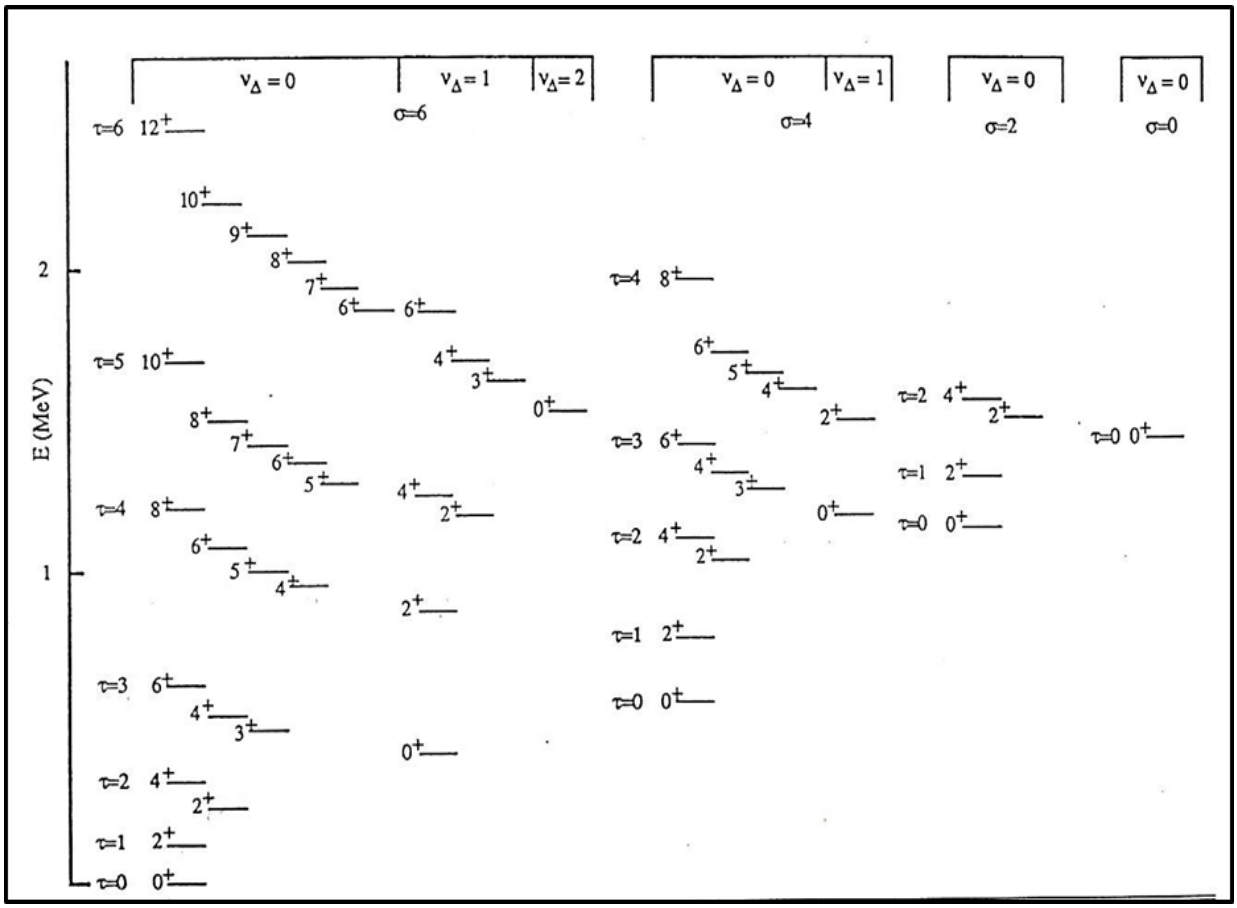

Figure (2.3) A typical spectrum and a quantum numbers for O(6) symmetry [77]

2.5 Transitions Regions in IBM-1

Many nuclei that have a transition property between two or three of the limits [78] can be represented by casten triangle, where the dynamical symmetries in vertices of the triangle are at the termini of the transition leg[79]. Figure (2.4) shows the casten triangle, that reveals three dynamical symmetries and transitional areas [80].

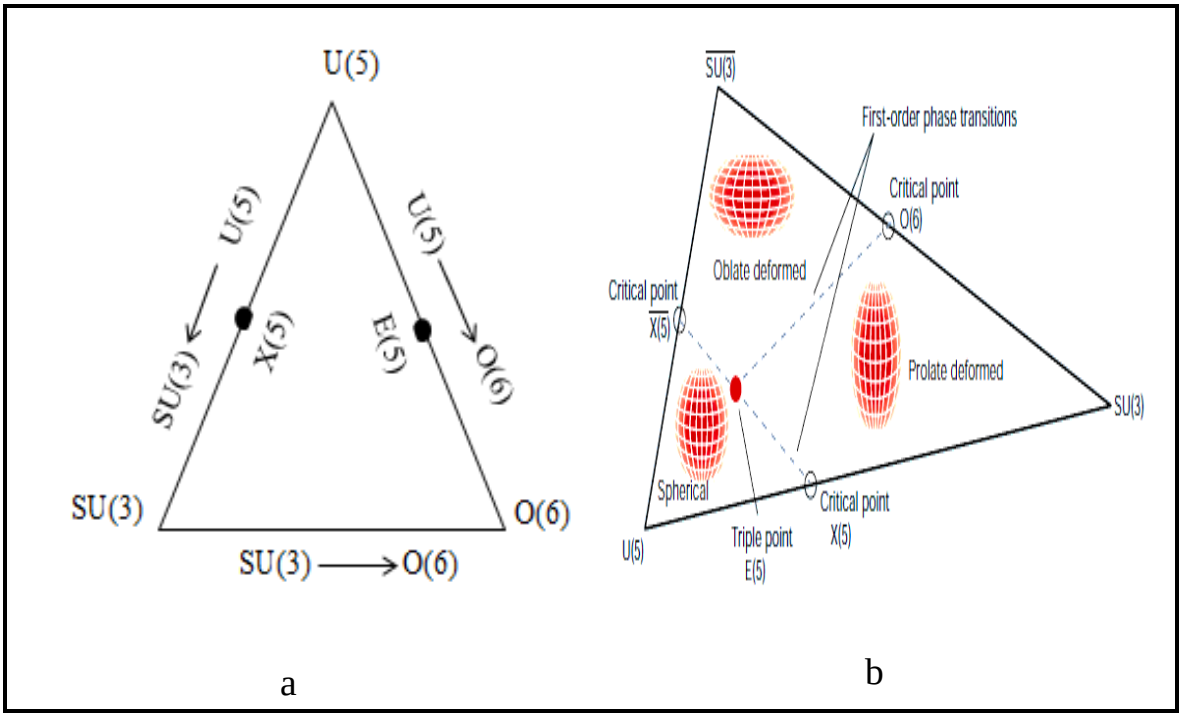

Figure (2.4) The Casten triangle [80]

Each peak in figure (b) represents a mathematical symmetry that is identical to one of the three forms shown above. Transition points and their crucial symmetries, as first-order phase transitions, are defined. Purposing that a nuclear triple point exists, this indicates that there is the second-order transition between a spherical and a prolate or oblate distorted nuclear shape [80]. Because the number of nuclei that may be characterized by these limitations is so small, the limits previously

discussed provide a set of analytical solutions that can be easily tested and because most nuclei share similar qualities between these limits that are called transition area, which can be divided into four types [81]:

2.5.1 Type 1: $\mathbf{U(5) \rightarrow O(6)}$

In this transition region, the nuclei have properties between the vibrational limit and the γ- unstable limit, and the Hamiltonian is [82]:

$$\hat{H} = \varepsilon \hat{n}_d + a_0 \hat{P}.\hat{P} + a_1 \hat{L}.\hat{L} + a_3 \hat{T}_3.\hat{T}_3 \qquad (2.39)$$

The properties of this limit depend on the ratio $(\varepsilon \hat{n}_d / a_0)$, when is large, the properties of this limit tend to be vibrational, while when is small, the properties tend to be γ- unstable.

2.5.2 Type 2: $\mathbf{O(6) \rightarrow SU(3)}$

In the transition region, the nuclei have properties between the rotational limit and the γ- unstable limit, and the Hamiltonian is [83]:

$$\hat{H} = a_0 \hat{P}.\hat{P} + a_1 \hat{L}.\hat{L} + a_2 \hat{Q}.\hat{Q} \qquad (2.40)$$

The properties of nuclei in this region are determined by the ratio (a_0/a_2). As a result, as the ratio increases, the properties become closer to the O(6) limit, and as the ratio decreases, the properties become closer to the SU(3) limit.

2.5.3 Type 3: $\mathbf{U(5) \rightarrow SU(3)}$

In the transition area, the nuclei have properties between the vibrational and rotational limits, and the Hamiltonian operator is as follows [84]:

$$\hat{H} = \varepsilon \hat{n}_d + a_1 \hat{L}.\hat{L} + a_2 \hat{Q}.\hat{Q} \quad (2.41)$$

The properties of nuclei in this region are determined by the ratio ($\varepsilon \hat{n}_d / a_2$). As a result, as the ratio increases, the properties become closer to the U(5) limit, and as the ratio decreases, the properties become closer to the SU(3) limit.

2.5.4 Type 4: $\mathbf{U(5) \rightarrow SU(3) \rightarrow O(6)}$

The nuclei of this type possesses the common properties between three limits and the Hamiltonian operator is written as follows [85]:

$$\hat{H} = \varepsilon \hat{n}_d + a_0 \hat{P}.\hat{P} + a_1 \hat{L}.\hat{L} + a_2 \hat{Q}.\hat{Q} + a_3 \hat{T}_3.\hat{T}_3 + a_4 \hat{T}_4.\hat{T}_4 \quad (2.42)$$

2.6 Potential Energy Surface Basis

As shown in equation(2.43), the potential energy surface (PES) ($E(N,\beta,\gamma)$) gives the nucleus a final shape that corresponds to the Hamiltonian function [60,86] :

$$E(N,\beta,\gamma) = \frac{\langle N,\beta,\gamma|H|N,\beta,\gamma\rangle}{\langle N,\beta,\gamma|N,\beta,\gamma\rangle} \quad (2.43)$$

The IBM energy surface is constructed using the expected value of the IBM-1 Hamiltonian with the coherent state ($|N,\beta,\gamma\rangle$) [87].

The state is a product of boson creation operators ($b_c^\dagger$), with

$$|N,\beta,\gamma\rangle = \frac{1}{\sqrt{N!}} \left(b_c^\dagger\right)^N |0\rangle \quad (2.44)$$

$$b_c^\dagger = (1+\beta^2)^{-\frac{1}{2}}\left\{s^\dagger + \beta\left[\cos\gamma\left(d_0^\dagger\right) + \sqrt{1/2}\,\sin\gamma\left(d_2^\dagger + d_{-2}^\dagger\right)\right]\right\} \quad (2.45)$$

The energy surface has been calculated as a function of (β) and (γ) [88]:

$$E(N,\beta,\gamma) = \frac{N\varepsilon_d}{(1+\beta^2)} + \frac{N(N+1)}{(1+\beta^2)^2}\,(a_1\beta^4 + a_2\beta^3\cos 3\gamma + a_3\,\beta^2 + a_4) \quad (2.46)$$

where the a_i's are related to the coefficients (C_L, ν_2, ν_0, u_2 and u_0) of equation(2.1).(β) is a measure representing the nucleus total deformation, when the shape is spherical ($\beta = 0$), and when the shape is deformed ($\beta \neq 0$), and (γ) is the amount of deviation from the focus symmetry and correlates with the nucleus, the shape is prolate if (γ = 0), and if (γ = 60) the shape becomes oblate [89]. The potential energy surface for three dynamical symmetries is given by the equations below [90]:

$$E(N,\beta,\gamma)\propto \begin{cases} U(5) & \varepsilon_d N\dfrac{\beta^2}{1+\beta^2} \\ SU(3) & kN(N-1)\dfrac{\frac{3}{4}\beta^4-\sqrt{2}\,\beta^3\cos 3\gamma+1}{(1+\beta^2)^2} \\ O(6) & \acute{k}N(N-1)\left(\dfrac{1-\beta^2}{1+\beta^2}\right)^2 \end{cases} \quad (2.47)$$

where ($k \propto a_2$ and $\acute{k} \propto a_0$) in equation (2.2). The scheme of contour lines and coaxial symmetries is shown in Figure (2.5).

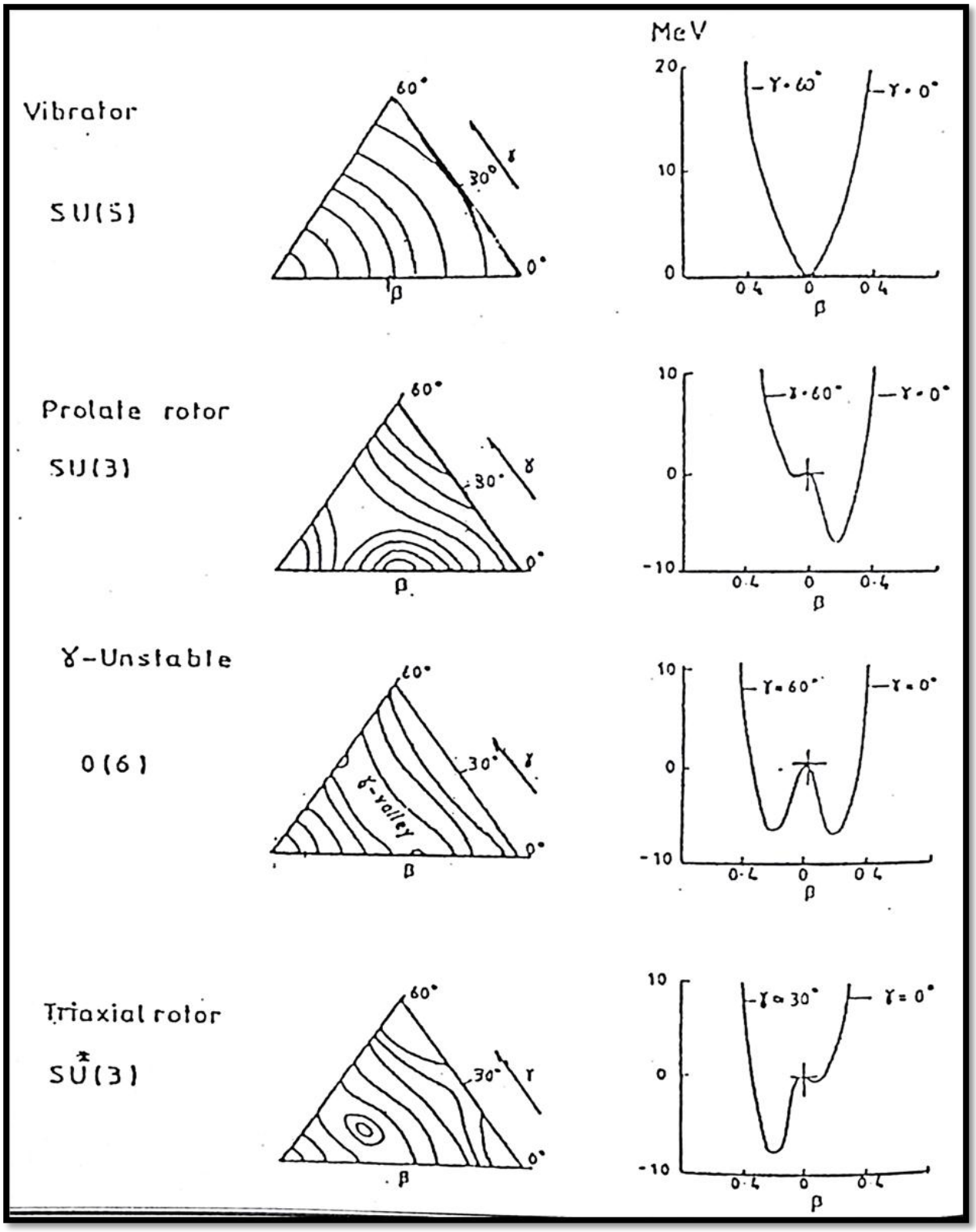

Figure (2.5) The ideal scheme of contour lines and coaxial Symmetries [91]

CHAPTER THREE

Results and Discussion

Chapter Three

Results and Discussion

3.1 Introduction

The IBM has been adopted to study some properties of the nuclear structure for even-even some isotones (^{194}Po,^{192}Pb, ^{190}Hg,^{188}Pt and ^{186}Os), has been studied low lying of the excited energy levels of these isotones and compared with available experiment data, specific the dynamic symmetries has been calculated through the energy ration between the (E_4^+/E_2^+ , E_6^+/E_2^+ , E_8^+/E_2^+ , E_0^+/E_2^+).The current work also studies the probability of occurrence of electrical transitions B (E2) through (IBMT) and its agreement with the practical possibility. Finally, the potential energy surface has been studied by IBMP program, to find out the deformation that occurs in the nucleus from the deviation of the contour lines and their aggregation in a specific area.

3.2 Scheme of work

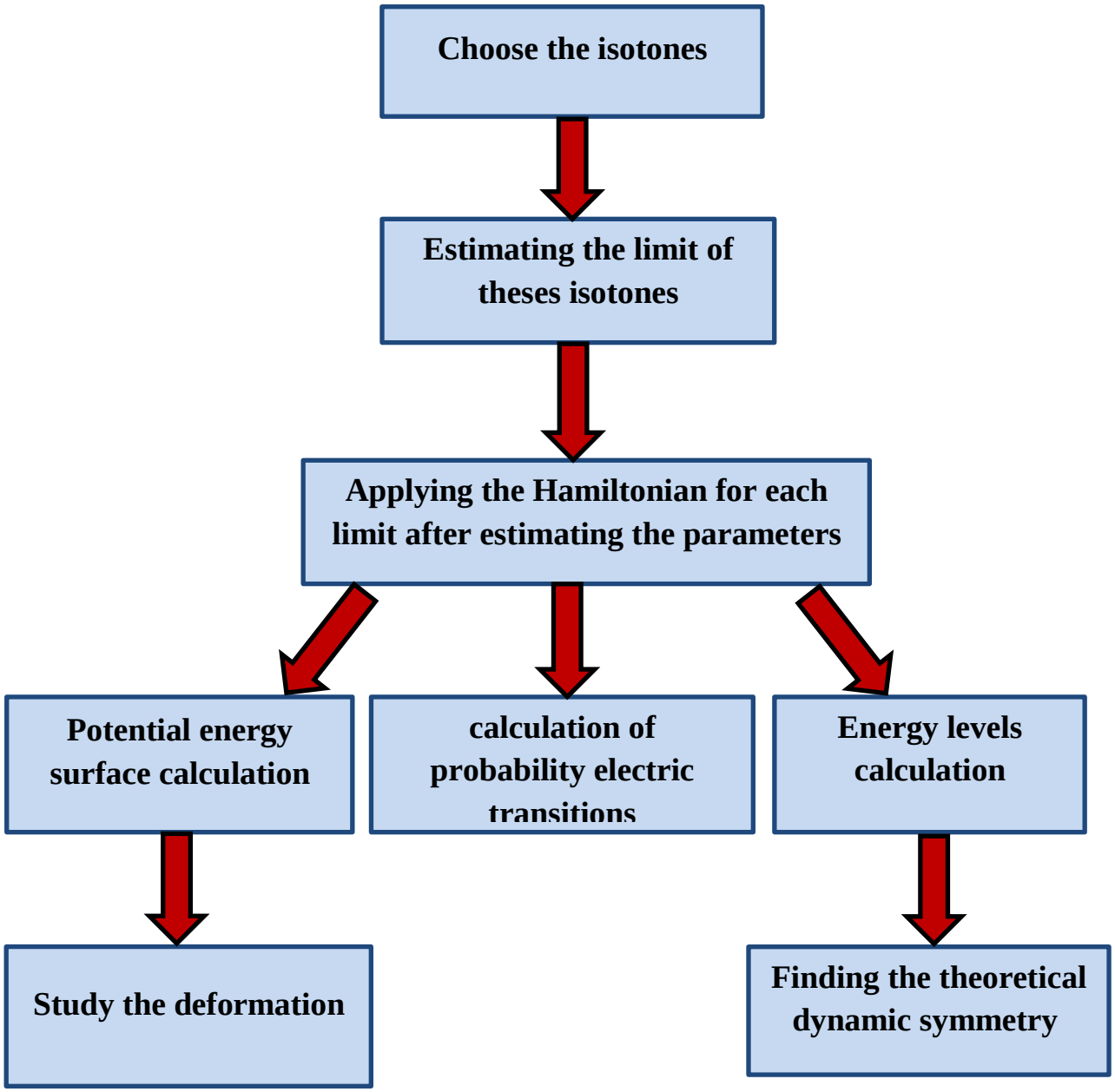

Figure (3.1) Schematic diagram of the experimental work.

3.3 Energy Levels

The dynamic symmetries through experimental and theoretical energy levels ratios ($E_{0_2^+}/E_{2_1^+}$, $E_{4_1^+}/E_{2_1^+}$, $E_{6_1^+}/E_{2_1^+}$, $E_{8_1^+}/E_{2_1^+}$) and comparison with the typical energy levels ratios for each limit [38,45] as shown in table (3.1).

Typical energy levels ratios for the vibration limit U (5), rotational limit SU(3) and γ- unstable O(6) denoted in Table (3.1) and the figure (3.2) is the comparison of $E_{0_2^+}/E_{2_1^+}$, figure (3.3) is the comparison of $E_{4_1^+}/E_{2_1^+}$, figure (3.4) is the comparison of $E_{6_1^+}/E_{2_1^+}$ and figure (3.5) is the comparison of $E_{8_1^+}/E_{2_1^+}$.

Table (3.1) Typical energy levels ratios for each limits [38, 45].

The Isotones	$E_{0_2^+}/E_{2_1^+}$		$E_{4_1^+}/E_{2_1^+}$		$E_{6_1^+}/E_{2_1^+}$		$E_{8_1^+}/E_{2_1^+}$	
	Exp.	**IBM**	**Exp.**	**IBM**	**Exp.**	**IBM**	**Exp.**	**IBM**
^{194}Po	--	3.5117	2.14	2.1455	3.5	3.4365	5.2	4.8732
^{192}Pb	0.9006	0.3295	1.58	1.6898	2.25	3.1518	2.69	4.1388
^{190}Hg	3.07	2.1992	2.5	2.4233	4.25	4.2699	5.92	6.5398
^{188}Pt	--	1.2792	2.52	2.5273	4.45	4.5822	6.7	7.1644
^{186}Os	7.73	7.1904	3.16	3.3327	6.33	6.9971	10.3	11.991

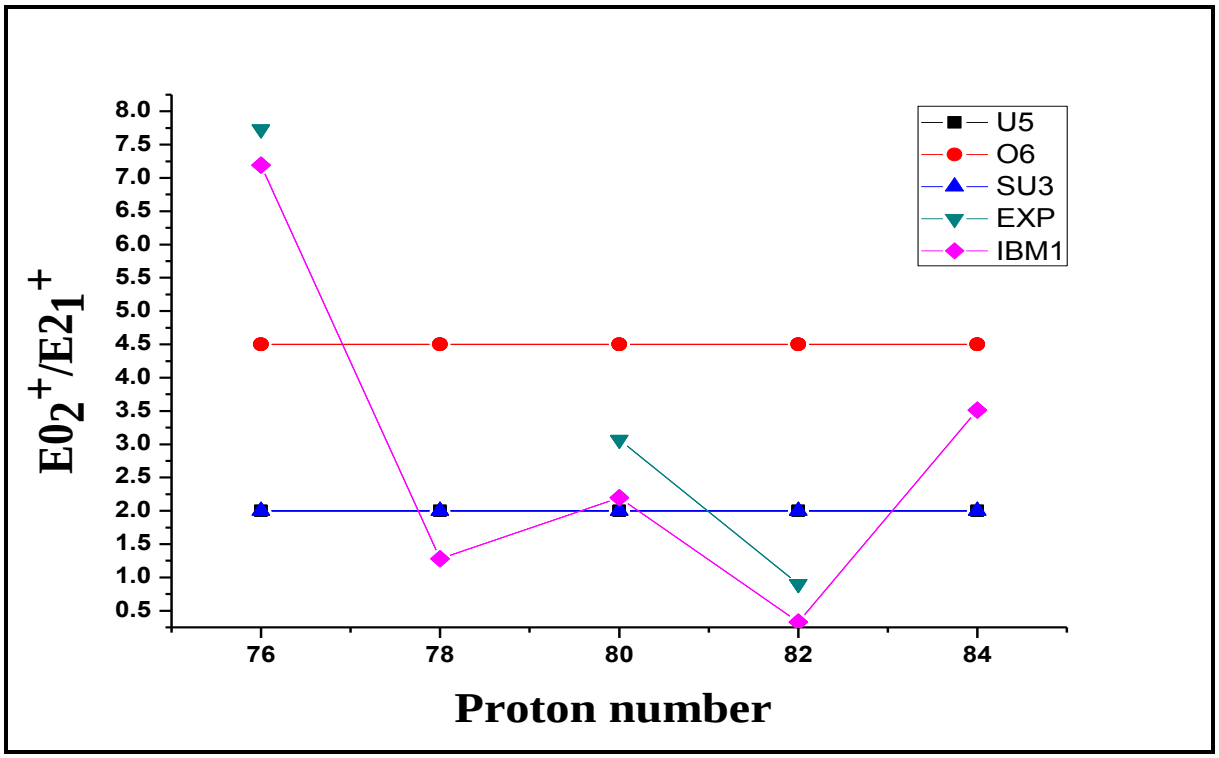

Figure (3.2) The comparison of $E_{0_2^+}/E_{2_1^+}$theoretically, experimentally and with typical values for every limit

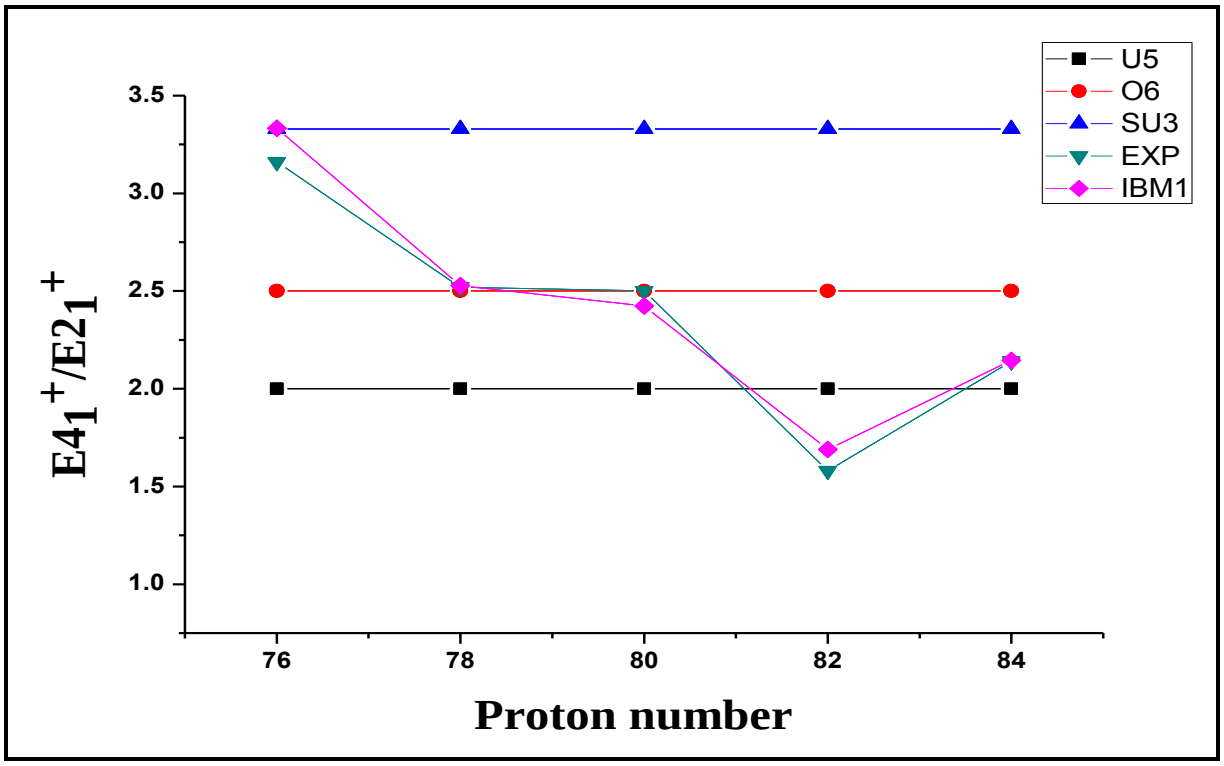

Figure (3.3) The comparison of $E_{4_1^+}/E_{2_1^+}$theoretically, experimentally and with typical values for every limit

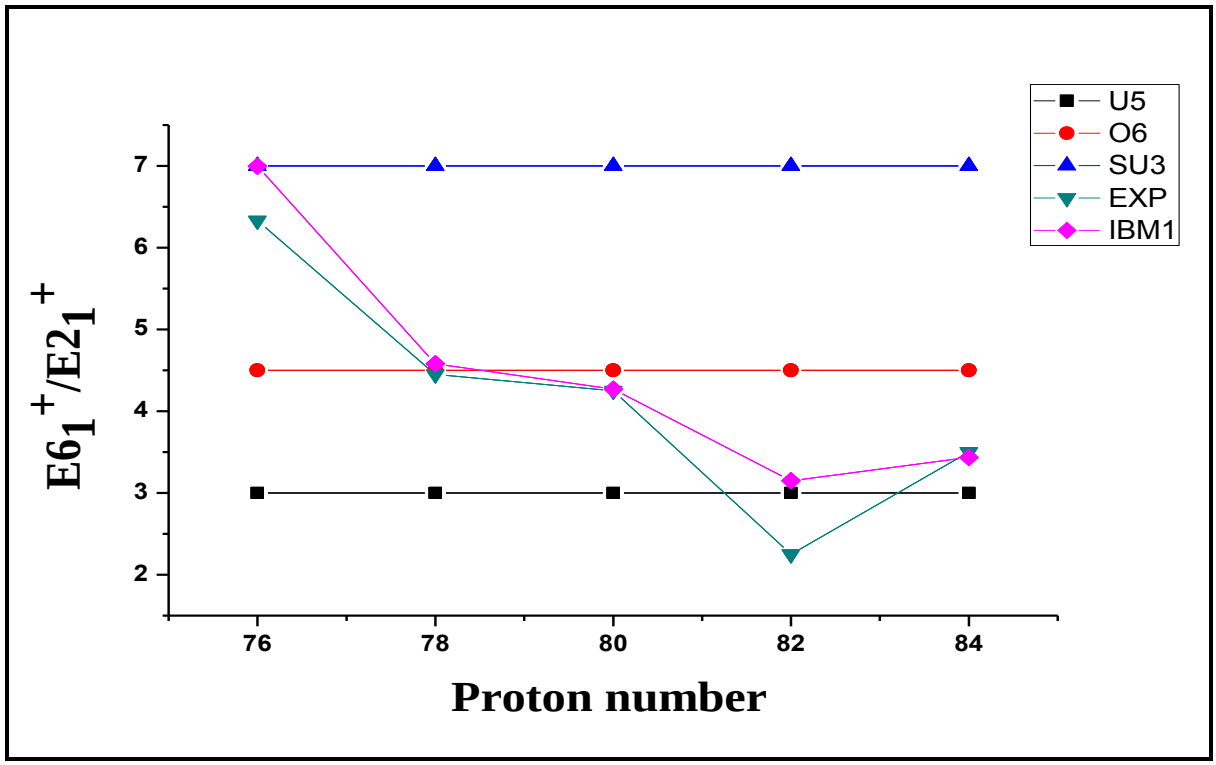

Figure (3.4) The comparison of $E_{6_1^+}/E_{2_1^+}$theoretically, experimentally and with typical values for every limit

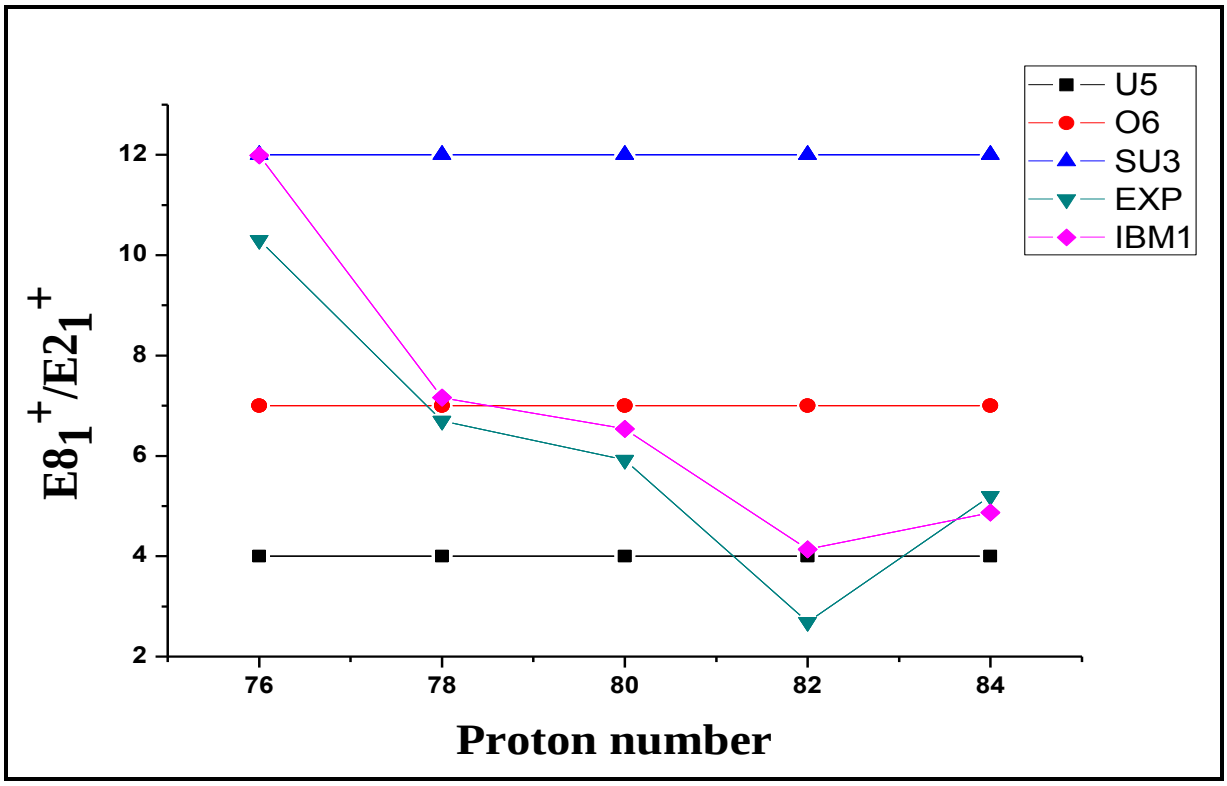

Figure (3.5) The comparison of $E_{8_1^+}/E_{2_1^+}$theoretically, experimentally and with typical values for every limit

Using IBM software, an examination of the experimental energy levels of (^{194}Po,^{192}Pb, ^{190}Hg,^{188}Pt and ^{186}Os) shows that it belongs to which limit.

Table (3.2), shows the parameters of the Hamiltonian that has been estimated in equation (2.2) to get best fit between the theoretical (IBM) result and experimental data taken from refs.[92].

Table (3.2) The Hamiltonian parameters used in the IBM-code for even-even isotones

The Isotones	N	EPS (Mev)	P. P (Mev)	L. L (Mev)	$Q.Q$ (Mev)	$T_3.T_3$ (Mev)	$T_4.T_4$ (Mev)	CHI	SO6
^{194}Po	9	0.0089	0	0.0052	0	0.0024	0.1533	0	1
^{192}Pb	8	0.6927	0	0.0120	0	0.1900	-0.0983	0	1
^{190}Hg	9	0	0.0916	0.0163	0	0.2273	0	0	1
^{188}Pt	10	0	0.0309	0.0143	0	0.1284	0	0	1
^{186}Os	11	0	0.3000	0.0180	-0.0141	0	0	-0.800000	1

Figure (3.6) shows a comparison between the theoretical and experimental energy levels for ^{194}Po where a number of uncertain levels is confirmed and at the same time giving some unknown energy levels in second band.

figure (3.7) shows a comparison between the theoretical and experimental energy levels for ^{192}Pb which giving many uncertain levels in second band.

Figure (3.8) and (3.9) are giving the energy levels for three bands to ^{190}Hg and ^{188}Pt.

Figure (3.10) denoted three bands for ^{186}Os and giving a good convergence for the experimental energy levels and theoretical one.

The best fit to the excited energy level, has been observed specially for the grand state band (i.e. 2_1^+, 4_1^+, 6_1^+,..) while the second and third band are found to show acceptable agreement.

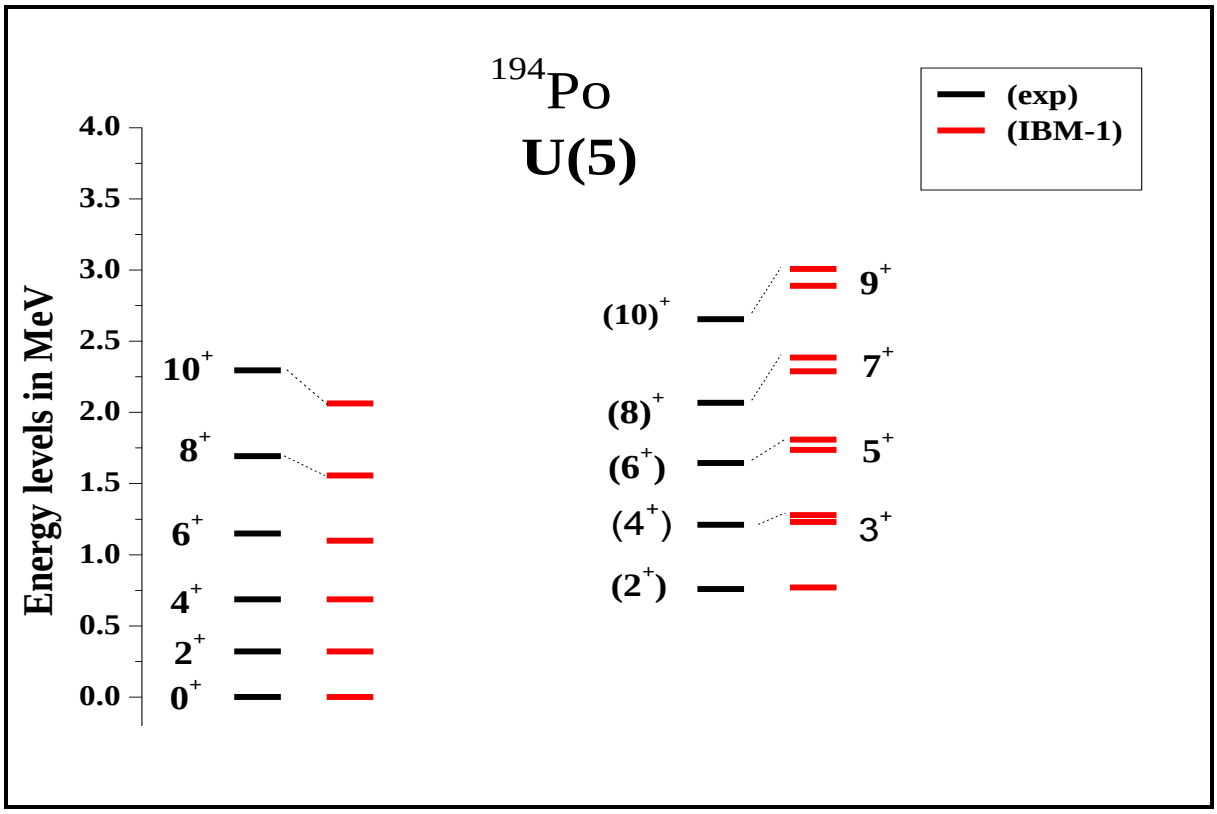

Figure (3.6): Comparison IBM-1 calculations with the experimental energy levels for ^{194}Po isotone

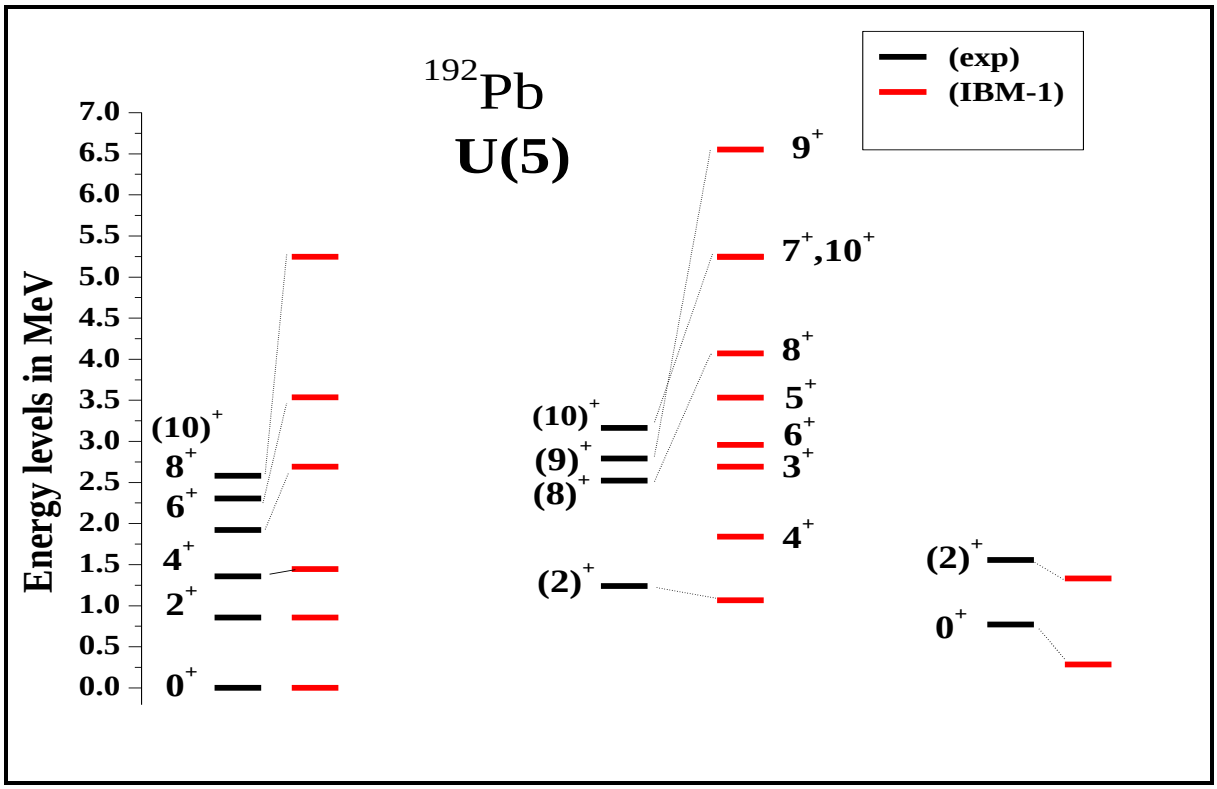

Figure (3.7): Comparison IBM-1 calculations with the experimental energy levels for ^{192}Pb isotone

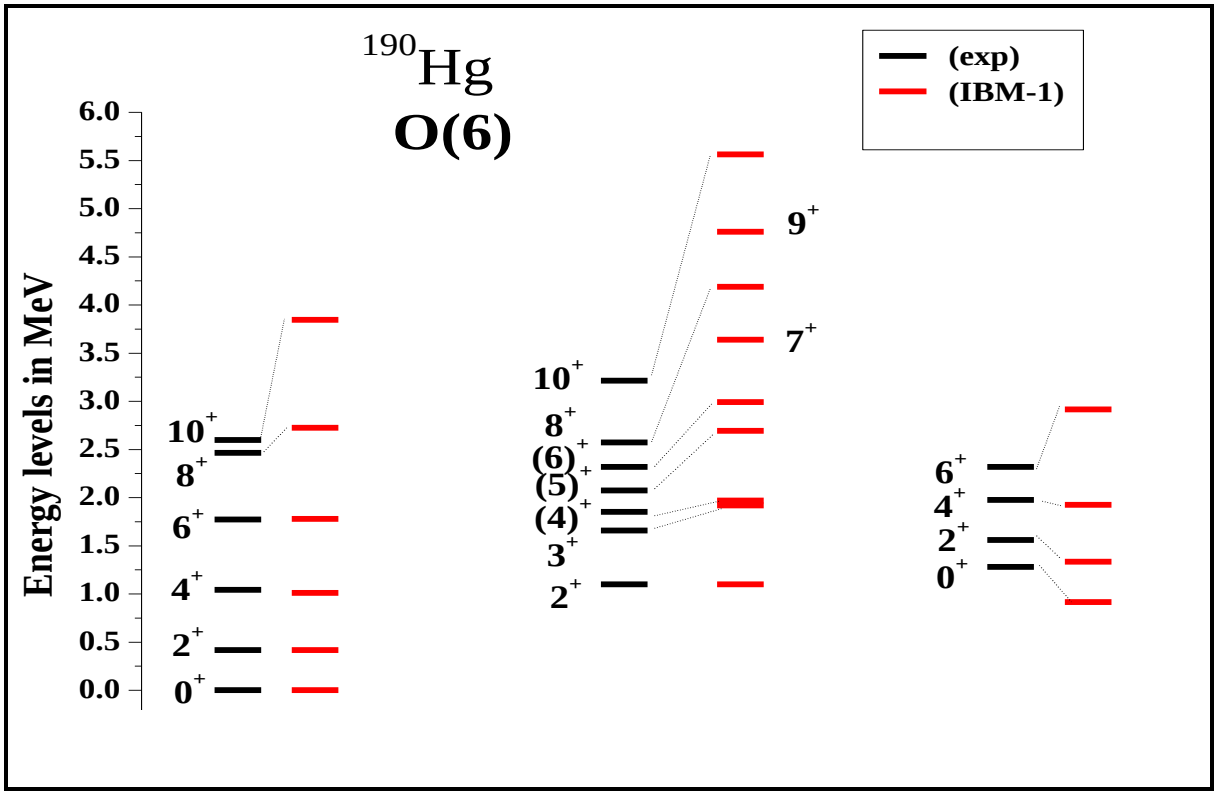

Figure (3.8): Comparison IBM-1 calculations with the experimental energy levels for ^{190}Hg isotone

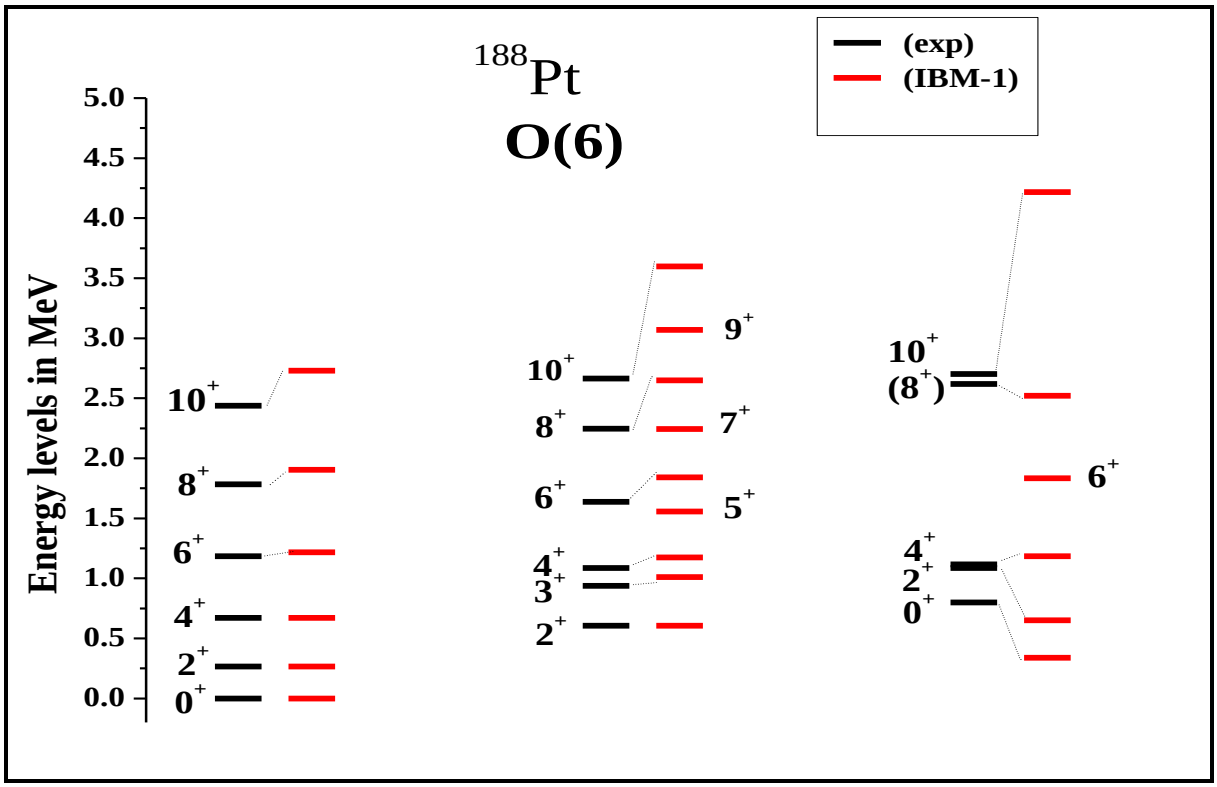

Figure (3.9): Comparison IBM-1 calculations with the experimental energy levels for ^{188}Pt isotone

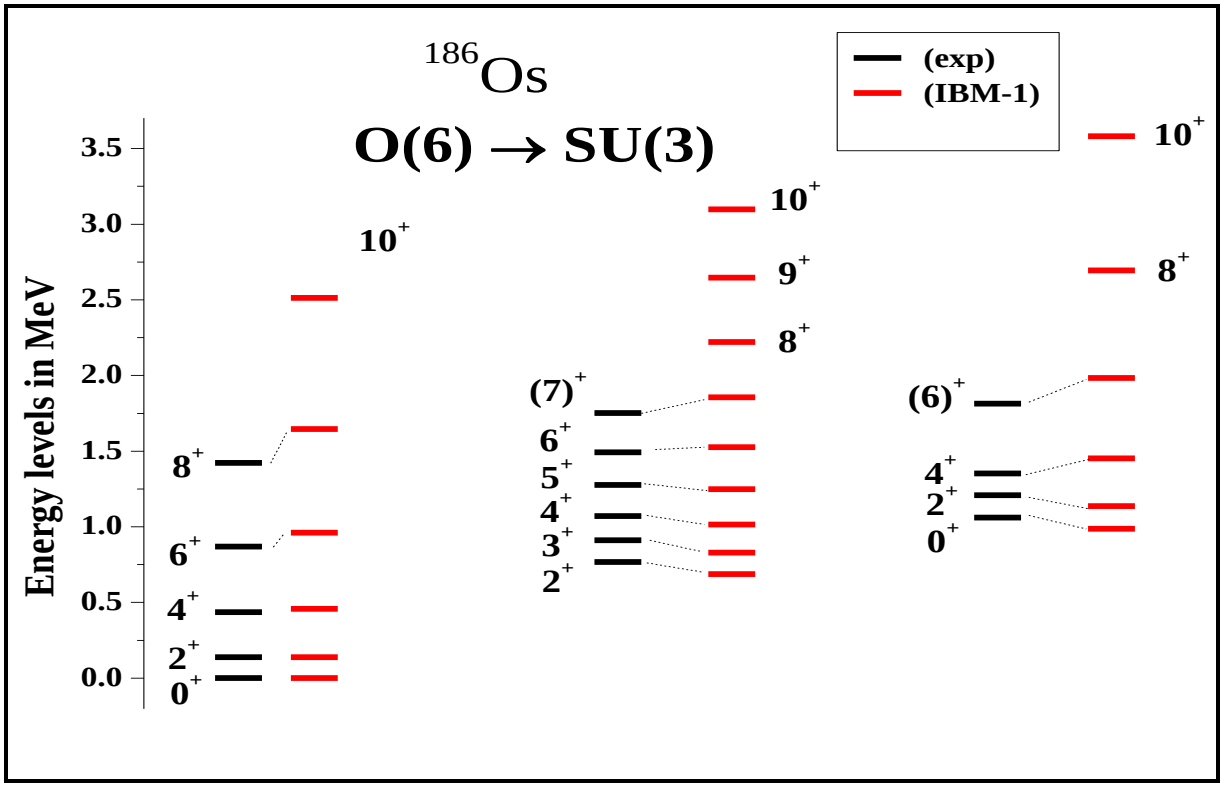

Figure (3.10): Comparison IBM-1 calculations with the experimental energy levels for ^{186}Os isotone

We estimated several energy levels for(^{194}Po, ^{192}Pb), and obtained from the results, there are unknown and questionable levels, which are a good match to the data from the ENSD weblink. These levels are (2_2, 3_1, 4_2, 5_1, 6_2, 7_1, 8_2, 9_1,10_2) for the ^{194}Po and (2_2, 3_1, 8_2, 9_1, 10_1,10_2) for the ^{192}Pb, and through the results we note that the nucleus is within the definition of U(5), where it is stable.

This nucleus, ^{190}Hg and ^{188}Pt of results, appears under O(6) limit, where we estimate several energy levels for this nucleus and get from the results, there are unknown and questionable levels, which are a good match to the data from the ENSD weblink. These are the levels (4_2, 5_1, 6_2, 7_1, 9_1) for the ^{190}Hg and (8_3,5_1, 7_1, 9_1, 6_3) for the ^{188}Pt.

Several energy levels for ^{186}Os are estimated where unknown and uncertain levels obtained from the results with good agreement with the experimental results. Some of these levels are (7_1,8_2, 9_1, 10_2,6_3) and through the results we note that the determination of this element is transitional O(6) - SU(3) .

3.4 Reduced Transition Probabilities B(E2) and Quadruple Moment $Q_{2_1^+}$

Many data can be gained by studying the reduced transition probabilities B(E2). The (IBMT-codes) are utilized and the values of (α_2, β_2) are evaluated in equation (2.21). The parameters (E2SD) and (E2DD) utilized in the current calculations are specified by normalizing the calculated values to the experimentally known ones and displayed in Table (3.3).

where

$$E2SD = \alpha_2 \tag{3.1}$$

$$E2DD = \sqrt{5}\beta_2 \tag{3.2}$$

The value of α_2 can be deduced from equation (2.24) to make the experimental values of $B(E2;2_1^+ \rightarrow 0_1^+)$.

The values of B(E2)$\downarrow$ are calculated using the beneficial relation [93]:

$$B(E2)\downarrow = \frac{(2I_f + 1)}{(2I_i + 1)} B(E2)\uparrow \tag{3.3}$$

where I_i and I_f are the total angular momentum for the initial and final state. Table (3.3) presents the values of (E2SD) and (E2DD) utilized in the present work with the experimental values of B(E2) taken from ref. [92], except ^{192}Pb, which is getting the value of B(E2) from ref. [94].

Table (3.3) The experimental values of B(E2) and the coefficients(E2SD, E2DD) for even-even used in the present work[92].

The isotones	$B(E2;\ 2_1^+ \rightarrow 0_1^+)$ e^2b^2	E2SD(eb)	E2DD(eb)
^{194}Po	0.594015	0.256906	-0.179833
^{192}Pb	0.122000	0.123490	-0.086441
^{190}Hg	0.292116	0.111729	0
^{188}Pt	0.569647	0.142634	0
^{186}Os	0.582404	0.132845	0

These bands have some probability of β and γ band so they are called (quasi β band γ band) all the momentum and parity for some energy level that had not been previously identified experimental for each isotones, are identified through this study.

A comparison between our experimental calculations and the recent available experimental data for B(E2) taken from refs. [92] are presented in tables (3.4-3.8) for ^{194}Po,^{192}Pb, ^{190}Hg,^{188}Pt and ^{186}Os respectively

Table (3.4) The experimental and calculated B(E2)↓ using IBMT-code and the quadrupole moment $Q(2_1^+)$ eb for ^{194}Po isotone.

$j_i^+ \rightarrow j_f^+$	B(E2) ↓e^2b^2	
	Exp. [92]	**IBM-1**
$2_1^+ \rightarrow 0_1^+$	0.594015	0.5939786
$2_1^+ \rightarrow 0_2^+$	--	0.2111923
$2_1^+ \rightarrow 2_2^+$	--	1.0559620
$2_1^+ \rightarrow 2_3^+$	--	0
$2_2^+ \rightarrow 0_1^+$	--	0
$2_2^+ \rightarrow 0_2^+$	--	0.0258711
$2_2^+ \rightarrow 2_1^+$	--	1.0559620
$2_2^+ \rightarrow 2_3^+$	--	0.2639904
$2_3^+ \rightarrow 0_1^+$	--	0
$2_3^+ \rightarrow 0_2^+$	--	0.6467768
$2_3^+ \rightarrow 2_1^+$	--	0
$2_3^+ \rightarrow 2_2^+$	--	0.2639905
$2_4^+ \rightarrow 0_1^+$	--	0
$2_4^+ \rightarrow 2_1^+$	--	0
$4_1^+ \rightarrow 2_1^+$	0.827617	1.0559620
$4_1^+ \rightarrow 2_2^+$	--	0.0105596
$4_2^+ \rightarrow 2_1^+$	--	0
$4_2^+ \rightarrow 2_2^+$	--	0.7259737
$4_3^+ \rightarrow 2_1^+$	--	0
$4_3^+ \rightarrow 2_2^+$	--	0
$Q\ (2_1^+ \rightarrow 2_1^+)$	--	-0.4021121

Table (3.5) The experimental and calculated B(E2)↓ using IBMT-code and the quadrupole moment $Q(2_1^+)$ eb for ^{192}Pb isotone.

$j_i^+ \rightarrow j_f^+$	B(E2) ↓e^2b^2	
	Exp. [92]	**IBM-1**
$2_1^+ \rightarrow 0_1^+$	0.122000	0.1219982
$2_1^+ \rightarrow 0_2^+$	--	0
$2_1^+ \rightarrow 2_2^+$	--	0
$2_1^+ \rightarrow 2_3^+$	--	0
$2_2^+ \rightarrow 0_1^+$	--	0
$2_2^+ \rightarrow 0_2^+$	--	0.0243996
$2_2^+ \rightarrow 2_1^+$	--	0
$2_2^+ \rightarrow 2_3^+$	--	0
$2_3^+ \rightarrow 0_1^+$	--	0
$2_3^+ \rightarrow 0_2^+$	--	0
$2_3^+ \rightarrow 2_1^+$	--	0
$2_3^+ \rightarrow 2_2^+$	--	0
$2_4^+ \rightarrow 0_1^+$	--	0
$2_4^+ \rightarrow 2_1^+$	--	0
$4_1^+ \rightarrow 2_1^+$	--	0
$4_1^+ \rightarrow 2_2^+$	--	0.0566420
$4_2^+ \rightarrow 2_1^+$	--	0.2134969
$4_2^+ \rightarrow 2_2^+$	--	0
$4_3^+ \rightarrow 2_1^+$	--	0
$4_3^+ \rightarrow 2_2^+$	--	0.0522850
$Q\ (2_1^+ \rightarrow 2_1^+)$	--	-0.1932879

Table (3.6) The experimental and calculated B(E2)↓ using IBMT-code and the quadrupole moment $Q(2_1^+)$ eb for ^{190}Hg isotone.

$j_i^+ \rightarrow j_f^+$	B(E2) ↓e^2b^2	
	Exp. [92]	**IBM-1**
$2_1^+ \rightarrow 0_1^+$	0.292116	0.2921109
$2_1^+ \rightarrow 0_2^+$	--	0
$2_1^+ \rightarrow 2_2^+$	--	0.3994679
$2_1^+ \rightarrow 2_3^+$	--	0
$2_2^+ \rightarrow 0_1^+$	--	0
$2_2^+ \rightarrow 0_2^+$	--	0
$2_2^+ \rightarrow 2_1^+$	--	0.3994680
$2_2^+ \rightarrow 2_3^+$	--	0
$2_3^+ \rightarrow 0_1^+$	--	0
$2_3^+ \rightarrow 0_2^+$	--	0.1922439
$2_3^+ \rightarrow 2_1^+$	--	0
$2_3^+ \rightarrow 2_2^+$	--	0
$2_4^+ \rightarrow 0_1^+$	--	0
$2_4^+ \rightarrow 2_1^+$	--	0
$4_1^+ \rightarrow 2_1^+$	0.1168466	0.3994678
$4_1^+ \rightarrow 2_2^+$	--	0
$4_2^+ \rightarrow 2_1^+$	--	0
$4_2^+ \rightarrow 2_2^+$	--	0.2288618
$4_3^+ \rightarrow 2_1^+$	--	0
$4_3^+ \rightarrow 2_2^+$	--	0
$Q\ (2_1^+ \rightarrow 2_1^+)$	--	-0.0000002

Table (3.7) The experimental and calculated B(E2)↓ using IBMT-code and the quadrupole moment $Q(2_1^+)$ eb for ^{188}Pt isotone.

$j_i^+ \rightarrow j_f^+$	B(E2) ↓e^2b^2	
	Exp. [92]	**IBM-1**
$2_1^+ \rightarrow 0_1^+$	0.569647	0.5696449
$2_1^+ \rightarrow 0_2^+$	--	0
$2_1^+ \rightarrow 2_2^+$	--	0
$2_1^+ \rightarrow 2_3^+$	--	0.7847149
$2_2^+ \rightarrow 0_1^+$	--	0
$2_2^+ \rightarrow 0_2^+$	--	0.3906137
$2_2^+ \rightarrow 2_1^+$	--	0
$2_2^+ \rightarrow 2_3^+$	--	0
$2_3^+ \rightarrow 0_1^+$	--	0
$2_3^+ \rightarrow 0_2^+$	--	0
$2_3^+ \rightarrow 2_1^+$	--	0.7847150
$2_3^+ \rightarrow 2_2^+$	--	0
$2_4^+ \rightarrow 0_1^+$	--	0
$2_4^+ \rightarrow 2_1^+$	--	0
$4_1^+ \rightarrow 2_1^+$	0.960080	0.7847148
$4_1^+ \rightarrow 2_2^+$	--	0
$4_2^+ \rightarrow 2_1^+$	--	0
$4_2^+ \rightarrow 2_2^+$	--	0.5289558
$4_3^+ \rightarrow 2_1^+$	--	0
$4_3^+ \rightarrow 2_2^+$	--	0
$Q\ (2_1^+ \rightarrow 2_1^+)$	--	0.0000002

Table (3.8) The experimental and calculated B(E2)↓ using IBMT-code and the quadrupole moment $Q(2_1^+)$ eb for ^{186}Os isotone.

$j_i^+ \rightarrow j_f^+$	B(E2) ↓e^2b^2	
	Exp. [92]	**IBM-1**
$2_1^+ \rightarrow 0_1^+$	0.582404	0.5089899
$2_1^+ \rightarrow 0_2^+$	--	0.0000134
$2_1^+ \rightarrow 2_2^+$	--	0.0635647
$2_1^+ \rightarrow 2_3^+$	--	0.0000288
$2_2^+ \rightarrow 0_1^+$	0.0637300	0.0380469
$2_2^+ \rightarrow 0_2^+$	--	0.0475088
$2_2^+ \rightarrow 2_1^+$	0.1482828	0.0635647
$2_2^+ \rightarrow 2_3^+$	--	0.0506919
$2_3^+ \rightarrow 0_1^+$	--	0.0000059
$2_3^+ \rightarrow 0_2^+$	--	0.3644842
$2_3^+ \rightarrow 2_1^+$	--	0.0000288
$2_3^+ \rightarrow 2_2^+$	--	0.0506919
$2_4^+ \rightarrow 0_1^+$	--	0.0000246
$2_4^+ \rightarrow 2_1^+$	--	0.0000373
$4_1^+ \rightarrow 2_1^+$	0.8455275	0.7145089
$4_1^+ \rightarrow 2_2^+$	--	0.0026048
$4_2^+ \rightarrow 2_1^+$	0.0201917	0.0172610
$4_2^+ \rightarrow 2_2^+$	0.4543133	0.2605792
$4_3^+ \rightarrow 2_1^+$	--	0.0000003
$4_3^+ \rightarrow 2_2^+$	0.1703675	0.0976296
$Q\ (2_1^+ \rightarrow 2_1^+)$	--	-1.8839560

A comparison between the experimental [92] and calculated $B(E2;2_1^+ \rightarrow 0_1^+)$ is displayed in Figure (3.11) and exhibits that the results are quite well for all isotones under study.

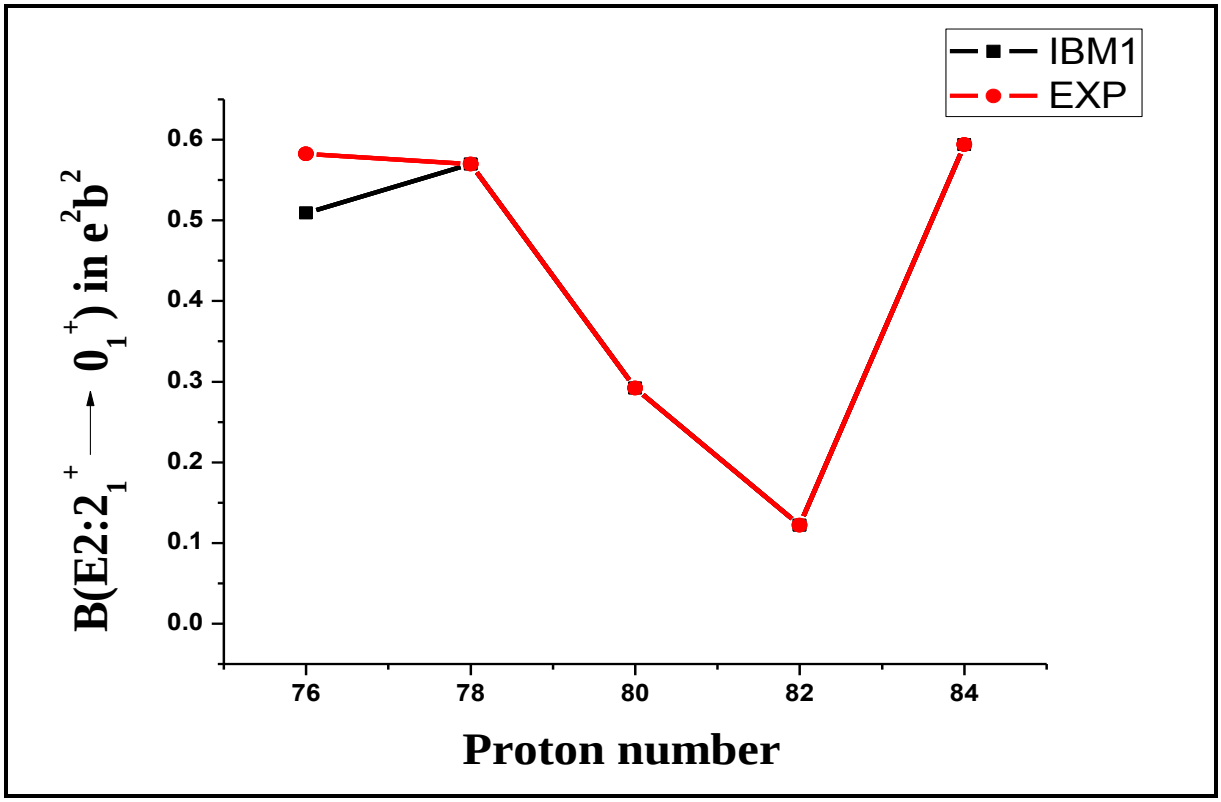

Figure (3.11) Comparison of the experimental and calculated $B(E2;2_1^+ \rightarrow 0_1^+)$ for isotones

The electric probability in figure (3.11) decreases with proton number to until reach magic numbers then increase with ^{194}Po number.

3.5 The B(E2) Branching Ratios

The B(E2) branching ratios $(R, R' and\ R'')$ are calculated in the present work for even-even (^{194}Po,^{192}Pb, ^{190}Hg,^{188}Pt and ^{186}Os) and it is known as the ratio between two reduced electric quadrupole transitions.

The significance of studying the branching ratios is to study the shape of the nucleus and dynamical symmetries they belong.

The calculated branching ratios and their equivalent experimental values are presented in Table (3.9).

Table (3.9):The branching ratio between two electric transitions.

The ratio	R		R'		R''	
The Isotones	Exp.[92]	IBM-1	Exp.[92]	IBM-1	Exp.[92]	IBM-1
^{194}Po	1.3932594	1.7777778	--	1.7777778	--	0
^{192}Pb	--	0	--	0	--	0
^{190}Hg	0.4000006	1.3675210	--	1.3675217	--	0
^{188}Pt	1.6853946	1.3775508	--	0	--	0
^{186}Os	1.4517886	1.4037781	0.2546047	0.1248840	--	0

3.6 Potential Energy Surface (P.E.S)

The potential energy surface is one of the nuclei properties, and it gives a definitive form of nuclei. The PES.FOR program is utilized to calculate the potential energy surface $E(N,\beta,\gamma)$. In this work, the potential energy surface is calculated from equations. (2.46,2.47) .

The Hamiltonian parameters that are used in the IBMP-code are shown in table (3.10). These parameters given from the equation of

potential energy surface. From output of IBM-program and compare with equation (2.46)

Table (3.10) The Hamiltonian parameters used in the IBMP-code for even-even isotones

The Isotones	ES (Mev)	ED (Mev)	A1 (Mev)	A2 (Mev)	A3 (Mev)	A4 (Mev)
^{194}Po	0.2569	-0.1798	0.0790	0	0	0
^{192}Pb	0.1235	-0.0864	-0.0510	0	0	0
^{190}Hg	0.1117	0	0.0230	0	-0.0460	0
^{188}Pt	0.1426	0	0.0080	0	-0.0150	0
^{186}Os	0.1328	0	0.0720	-0.0240	-0.2060	0

Figures (3.12-3.16) represent the potential energy surface for (^{194}Po,^{192}Pb, ^{190}Hg,^{188}Pt and ^{186}Os) respectively, as contour lines and symmetric shape of prolate if ($\gamma = 0$), and oblate if ($\gamma = 60$).

These figures show that there are symmetry both side in ^{194}Po, ^{192}Pb, ^{190}Hg, ^{188}Pt but there isn't in ^{186}Os which mean there is deformation in this nucleus. The figures of contour lines of potential energy surface compared with typical one in figure (2.5), so note that there is deformation in ^{186}Os.

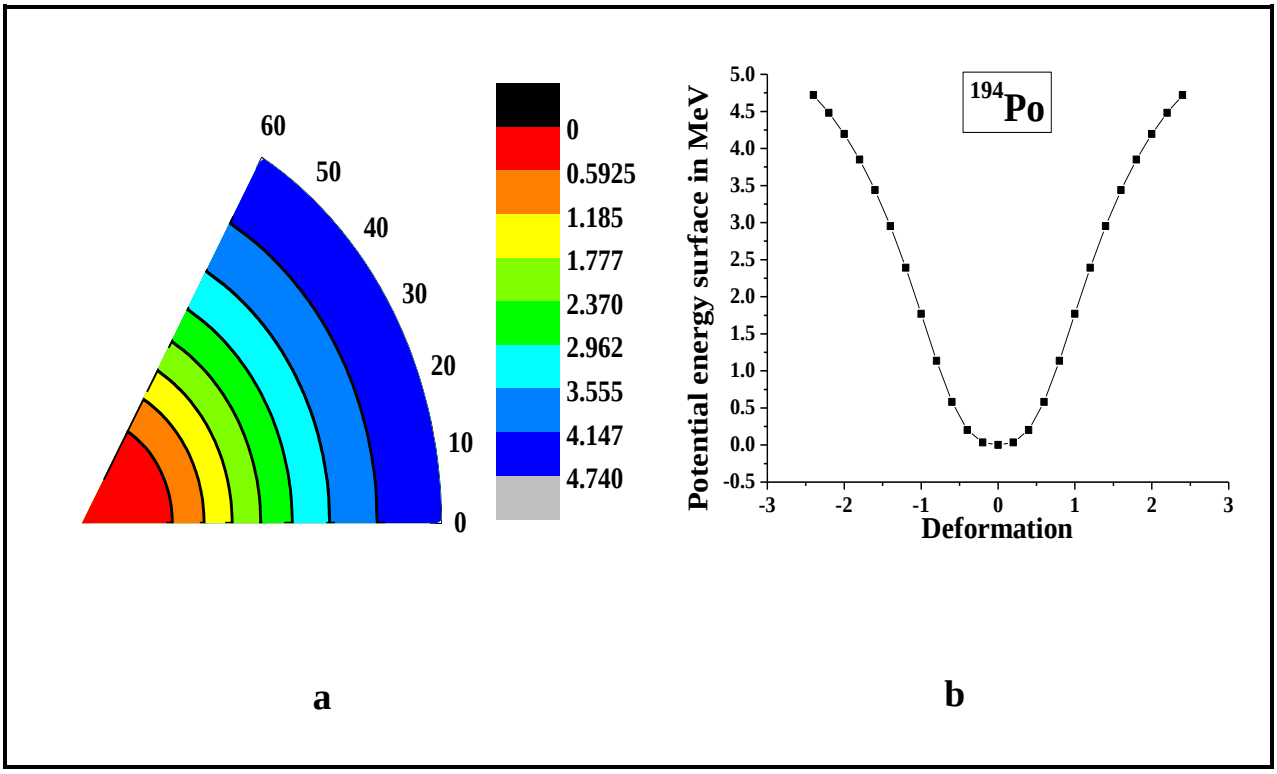

Figure (3.12): Potential energy for ^{194}Po, (a) contour (b) symmetric

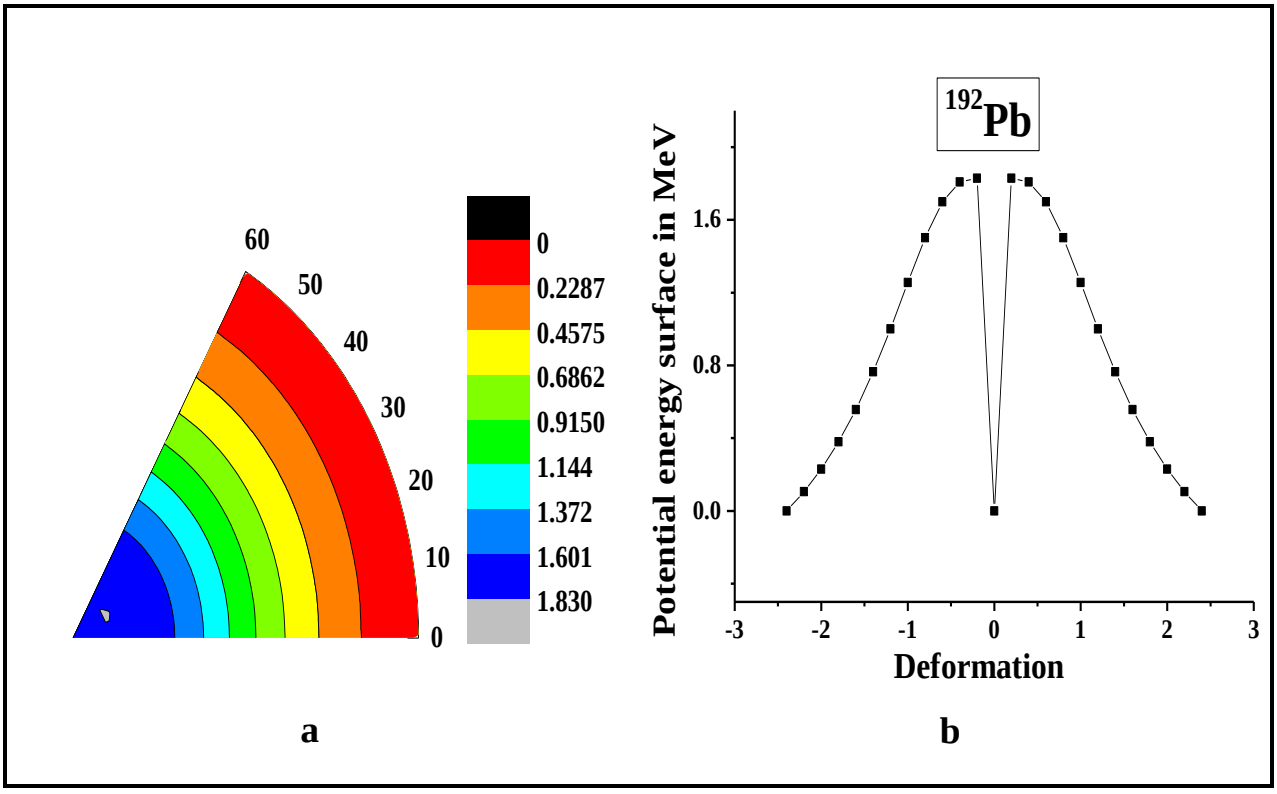

Figure (3.13): Potential energy for ^{192}Pb, (a) contour (b) symmetric

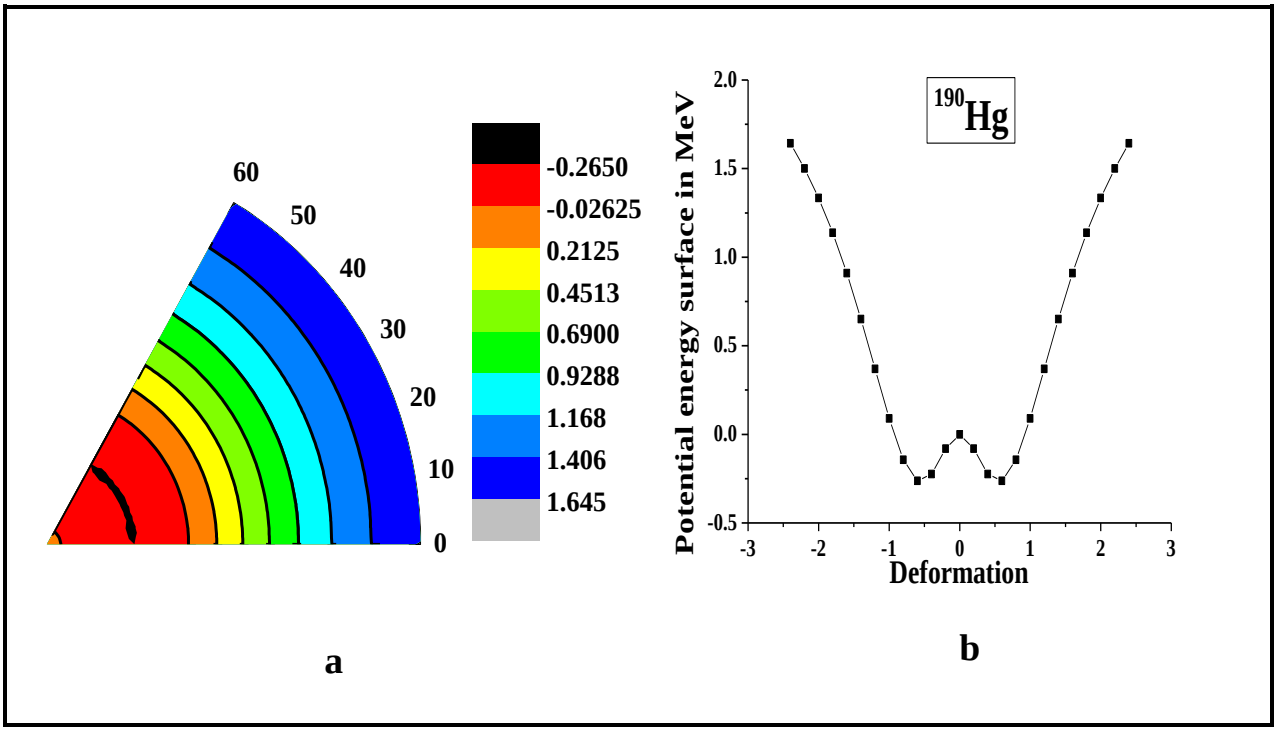

Figure (3.14): Potential energy for ^{190}Hg, (a) contour (b) symmetric

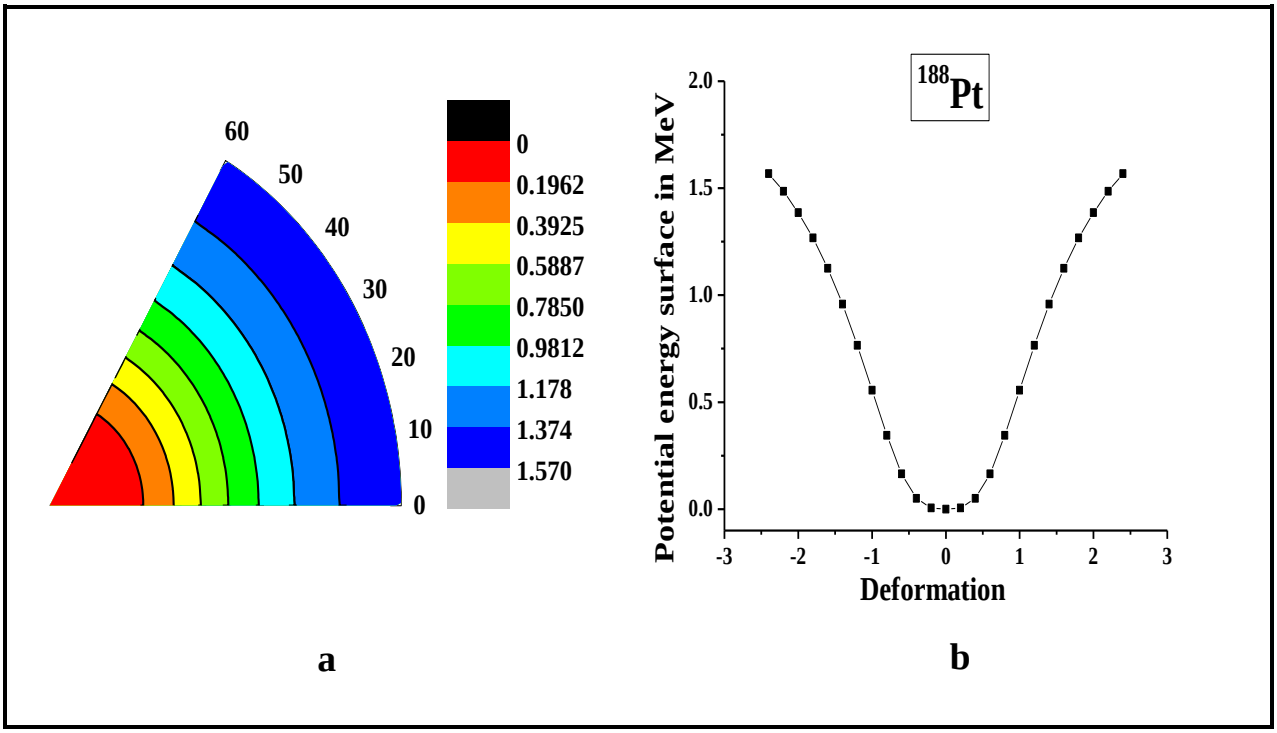

Figure (3.15): Potential energy for ^{188}Pt, (a) contour (b) symmetric

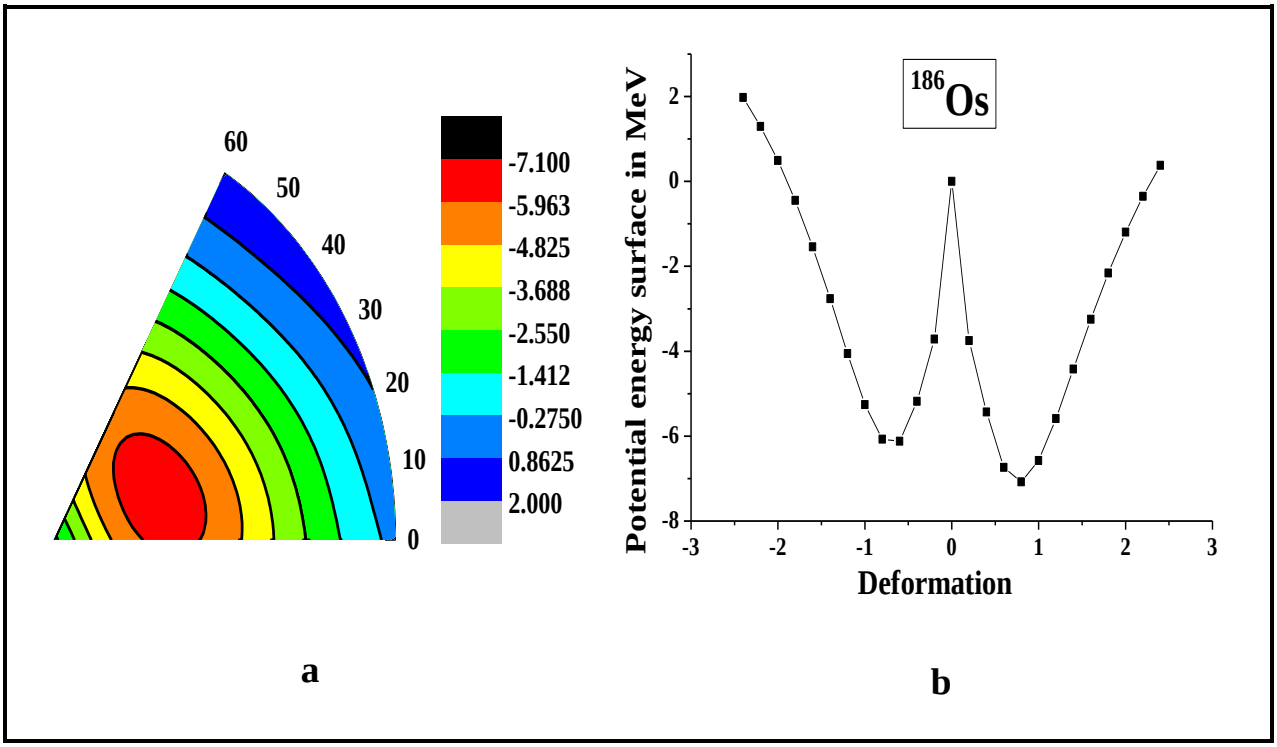

Figure (3.16): Potential energy for ^{186}Os, (a) contour (b) symmetric

Figure (3.12), the minimum value of the potential energy surface equal (0) Mev at β = (0) and it almost does not appear in the contour shape, then the value of the potential energy increases in the following regions to reach its highest value at (4.740) Mev at $\beta = (2.4),\ 0 \leq \gamma \leq 60$.

Figure (3.13), the minimum value of the potential energy surface (0) Mev at β = (2.4) and it almost does not appear in the contour shape, then the value of the potential energy increases in the following regions to reach its highest value at (1.83) Mev at $\beta = (0.2), 0 \leq \gamma \leq 60$.

Figure (3.14), the minimum value of the potential energy surface (-0.2650) Mev at β = (0.6) and after that it returns to zero at β = (0) in $0 \leq \gamma \leq 30$ and is reflected in $30 \leq \gamma \leq 60$, then the value of the potential energy increases in the following areas to reach its highest value is at(1.645) Mev with β = (2.4).

Figure (3.15), the minimum value of the potential energy surface (0)Mev at β = (0) and it almost does not appear in the contour shape, then the value of the potential energy increases in the following regions to reach its highest value at (1.570) Mev at $\beta = (2.4), 0 \leq \gamma \leq 60$.

In the figure (3.16) it appears that the two sides are not alike, as on the left side at $0 \leq \gamma \leq 30$ the highest value of the potential energy surface (2)Mev at β = (-2.4) and its lowest value (-6.12238) Mev at β = (-0.6), after which it returns to zero. On the right at $30 \leq \gamma \leq 60$, the highest value is (0.37762)Mev at β = (2.4) and the lowest at (-7.10)Mev at β = (0.8).

CHAPTER FOUR

Conclusions and Future Works

Chapter Four

Conclusions and Future Works

4.1 Energy Levels for Even - Even Isotones

1. The spin and parity of many excited energy levels were not confirmed in the experimental data, where we able to estimate the most probable spin, parity of the energy states.
2. Shape coexistence (dynamic symmetries) was determined in these isotones, where their deformation increase with proton number except the magic shell nuclei.

4.2 Reduced Transition Probability B(E2) and Electric Quadrupole Moment $Q(2_1^+)$

1. The study of the reduced transition probability $\mathrm{B(E2;}\ 2_1^+ \rightarrow 0_1^+)$, decreases as the proton number increase, and this is a key signature that the nuclei deformation becomes less when near to the closed shell and becomes stable then increases again when far from it. The calculations of B(E2) values display a good agreement with the available experimental data. However, in some cases, they can be higher or lower than the experimental values, due to the deformation effects of these nuclei.

2. The ratios of the reduced transition probabilities R, $R'$and R'' are in agreement both experimentally and theoretically and are in consistence with their ideal corresponding limits as displayed in table (3.9).

3. The study of the quadrupole moment $Q_{2_1^+}$ for (^{186}Os) is more prolate distorted shape than the other isotones under study and the prolate perversion from spherical symmetry reduces with the increase of mass number.

4.3 Potential Energy Surface (P.E.S)

1. The axially symmetric for the isotones ^{194}Po,^{192}Pb is agreeing with the typical axially symmetric of the U(5) limit. The deformation does not continue, it is just vibrational surface around the spherical shape results from phonons interaction.

2. In the isotone ^{192}Pb, we could not get a good match as in the rest of the isotones, because it contains a closed shell of protons and the number of bosons comes from neutrons only. Therefore the fitting energy levels were getting from U(5) Hamiltonian for low energy levels only, but there are difference for high levels.

3. The axial symmetry of the radioactive isotones ^{190}Hg, ^{188}Pt is found to be compatible with the typical axial symmetry of the O(6) term, where its shape is irregular as the contour lines gather in one place and decrease in another, meaning that the distribution of the contour lines is uneven on the surface of the nucleus.

4. The ^{186}Os is highly distorted where the distribution of the contour lines on the surface of the nucleus is random and irregular, and there isn’t symmetry in both sides, this means that the potential

distribution is not equal across the surface of the nuclei and belongs to rotational limit O(6)-SU(3).

5. Potential energy surface is giving us a good perception to get the shape of the nuclei from the contour lines. The symmetric figures explain the kind of the symmetry in the nuclei. We can confirm that the predictions for the limits of our isotones which were determined are correct.

4.4 Future Works

It seems clear that further work is required to find more identifiable features in this mass region, therefore we suggest the following:

1. This work can be repeated but instead of using the first versions of IBM the extended version IBM-2 can be employed to perform the calculation for the isotopes which may enhance the calculations.

2. Study the nuclear structure for even-odd isotones by using (IBFM-1) and (IBFM-2) model.

References

References:

[1] H. A. Bethe and R. F. Bacher, "Nuclear physics A. Stationary states of nuclei", Reviews of Modern Physics, 8(2), 82, (1936).

[2] J. M.Blatt and V. F. Weisskopf, "Theoretical nuclear physics", Courier Corporation, (1991).

[3] D. J. Rowe, "Nuclear collective motion: models and theory",World Scientific, (2010).

[4] M. G. Mayer," Nuclear configurations in the spin-orbit coupling model. i. empirical evidence", Physical Review, 78(1), 16, (1950).

[5] A. N. Bohr and B. R. Mottelson, "Nuclear Structure (In 2 Volumes)", World Scientific Publishing Company, (1998).

[6] P. Van Isacker, "Symmetries of the interacting boson model", Frontiers of Physics, 13(6), 132107, (2018)

[7] R. F. Casten,"Nuclear structure from a simple perspective", Oxford University Press on Demand, 23, (2000).

[8] D. Wilmsen, "Nuclear structure studies with neutron-induced reactions: fission fragments in the N= 50-60 region, a fission tagger for FIPPS, and production of the isomer Pt-195m", Ph.D Thesis, University of Normandie, (2017).

[9] W. E. Meyerhof, "Elements of nuclear physics", New York: McGraw-Hill, (1967).

[10] R. F. Casten, "Nuclear structure from: build complex structures", Oxford University Press, Inc., (1990).

[11] S. S. Wong, "Introductory nuclear physics", American Association of Physics Teachers, (1998).

[12] M. A. Caprio, "Structure of collective modes in transitional and deformed nuclei", Yale University, (2003).

[13] A. K. Varshney, "Nuclear structure studies in even-even medium and heavy nuclei", Ph.D, Thesis, Aligarh Muslim University, (1988).

[14] B. R. Muhyedeen, "On heuristic viewpoints concerning the mass, energy and light concepts in quantum physics", European Journal of Scientific Research, 22(4), 584-601, (2008).

[15] K. S. Krane, "Introductory nuclear physics", John Willey and Sons, (1991).

[16] A.Vértes, S.Nagy and Z.Klencsár, "Handbook of nuclear chemistry ", Springer Science and Business Media, (2011).

[17] O. Haxel, J. H. D. Jensen and H. E. Suess, "On the magic numbers in nuclear structure", Physical Review, 75(11), 1766, (1949).

[18] S. S. Wong, "Introductory nuclear physics" , John Wiley and Sons. (2008).

[19] A. Bohr and B.R. Mottelson, " Interpretation of isomeric transitions of electric quadrupole type", Physical Review, 89(1), 316, (1953).

[20] M. Brucer, "Nuclear medicine begins with a boa constrictor", Journal of Nuclear Medicine, 19(6), 581-598, (1978).

[21] E. Frieden, "The chemical elements of life", Scientific American, 227(1), 52-64, (1972).

[22] D. R. Lide, "Handbook of chemistry and physics", CRC press. (2004).

[23] Y. Shi, F. R. Xu, H. L. Liu and P. M. Walker, "Multi-quasiparticle excitation: Extending shape coexistence in A~ 190 neutron-deficient nuclei", Physical Review C, 82(4), 044314, (2010).

[24] K. Nomura, T. Otsuka, R. Rodríguez-Guzmán, L. M. Robledo, P. Sarriguren, P. H. Regan and Z. Podolyák, "Spectroscopic calculations of the low-lying structure in exotic Os and W isotopes", Physical Review C, 83(5), 054303, (2011).

[25] Y. Zhang, F. Pan, Y. X. Liu, Y. A. Luo and J. P. Draayer, "Analytically solvable prolate-oblate shape phase transitional description within the SU(3) limit of the interacting boson model", Physical Review *C*, *85*(6), 064312, (2012).

[26] F. I. Sharrad, H. Y. Abdullah, N. Al-Dahan, N. M. Umran, A. A. Okhunov and Kassim, H. A. , "Low-lying states of ^{184}W and ^{184}Os nuclei", Chinese Physics C, 37(3), 034101, (2013).

[27] H. N. Hady, "Transitions symmetries shape in $^{176\text{-}196}$ Pt isotopes with interacting boson model", Journal of University of Babylon, 21(6), (2013).

[28] H. H. Kassim and F. I. Sharrad, "O (6) symmetry of even $^{186-\ 198}$Pt isotopes under the framework of interacting boson model (IBM-1)", International Journal of Science and Research (IJSR), 3, 2189, (2014).

[29] J. E. García-Ramos, K. Heyde, L. M. Robledo and R. Rodríguez-Guzmán, "Shape evolution and shape coexistence in Pt isotopes: Comparing interacting boson model configuration mixing and

Gogny mean-field energy surfaces", Physical Review C, 89(3), 034313, (2014).

[30] J. E. García-Ramos and K. Heyde," The influence of intruder states in even-even Po isotopes", In AIP Conference Proceedings, 1681, (1), 040008, (2015).

[31] J. E. García-Ramos and K. Heyde, "Nuclear shape coexistence in Po isotopes: An interacting boson model study", Physical Review C, 92(3), 034309, (2015).

[32] K. A. Hussain, M. K. Mohsin and F. I.. Sharrad, "Calculation of the positive parity Yrast bands of $^{190-198}$Hg Nuclei", Ukrainian Journal of Physics, 62(8), 653-653, (2017).

[33] F. Pan, S. Yuan, Z. Qiao, J. Bai, Y. Zhang and J. P. Draayer, "γ-soft rotor with configuration mixing in the O (6) limit of the interacting boson model", Physical Review C, 97(3), 034326, (2018).

[34] M. M. Hammad, S. M.Fawaz, M. N. El-Hammamy, H. A. Motaweh and S. B. Doma, "q-deformed vibrational limit of interacting boson model", Journal of Physics Communications, 3(9), 085019, (2019).

[35] Gh. A. Jaber and M. K. Muttaleb, "Studying the breaking symmetry for O (6) even Hg isotopes in interacting boson model (1 and 2)", In AIP Conference Proceedings, 2144(1), 030014, (2019)

[36] J. Kotila, "Comparison of microscopic interacting boson model and quasiparticle random phase approximation 0νββ decay nuclear matrix elements", Frontiers in Astronomy and Space Sciences, 8, 42 (2021).

[37] A. J. Majarshin, Y. A. Luo, F. Pan, H. T. Fortune and J. P. Draayer, "Nuclear structure and band mixing in ^{194}Pt", Physical Review C, 103(2), 024317, (2021).

[38] A. Arima and F. Iachello, "The Interacting Boson Model", Cambridge University Press, Cambridge, UK, (1987).

[39] W. Pfeifer, "An introduction to the interacting boson model of the atomic nucleus" , arXiv, (1998).

[40] F. Iachello and P. Van Isacker, "The interacting boson-fermion model", Cambridge University Press, (1991).

[41] J. Rainwater, " Nuclear Energy Level Argument for a Spheroidal Nuclear Model", Physical Review, 79(3), 432, (1950).

[42] I. Hossain, I. M. Ahmed, F. Sharrad, H. Y. Abdullah, A.D. Salman and N. Al-Dahan, "Yrast states and B(E2) values of even $^{100–102}$Ru isotopes using interacting boson model (IBM-1)", Chiang Mai J Sci., 42, 996–1004, (2015).

[43] H. R. Yazar and I. Uluer, "Negative parity states and some electromagnetic transition properties of even-odd erbium isotopes", Physical Review C, 75(3), 034309, (2007) .

[44] A. Arima, and F. Iachello, "The interacting boson model", Annual Review of Nuclear and Particle Science, 31(1), 75-105, (1981).

[45] R. F. Casten, and D.D Warner, "The Interacting Boson Approximation", Reviews of Modern Physics, 60(2), 389-406, (1988).

[46] J. Basdevant, J. Rich and M. Spiro, "Fundamentals in Nuclear Physics", Springer Science and Business Media, (2004).

[47] J. Proskurins, "The Study of Nuclear Shape Phase Transitions and Quantum Chaos in The Frameworks of Geometrical and Algebraic Models of Even-Even Nuclei", Ph.D, Thesis, University of Latvia, (2010).

[48] I. M. Ahmed and M. I. M. Mustafa, " The Evolution of ^{146}Nd-^{156}Nd Isotope States under the Framework of BM, IBM-1, IVBM and D-G", Zanco Journal of Pure and Applied Sciences, 28(6), 21-31, (2016).

[49] A. Sethi, N. M. Hintz, D. N. Mihailidis, A. M. Mack ,M. Gazzaly, K. W.Jones and D. Goutte," Inelastic proton scattering from Pt isotopes and the interacting boson model", Physical Review C, 44(2), 700, (1991).

[50] W. T. Chou, D. S. Brenner, R. F. Casten and R. L. Gill, "Level Lifetime Measurements and The Structure of Neutron-Rich ^{78}Ge", Physical Review C, 47(1), 157–162, (1993).

[51] J. Engel, and F. Iachello, "Interacting boson model of collective octupole states Pt. 1. The rotational limit", Nucl. Phys.A;(Netherlands), 472(1), (1987).

[52] Gh. A. Jaber and M. K. .Al-Jnaby, "Nuclear Structure for Some Even-Even (Kr, Xe, Hg) Nuclei Using IBM1,2", Ph.D. thesis, University of Babylon, (2020).

[53] Gh. A. Jaber and M. K. Muttaleb, "Studying the Isotopes nearby Closed Shell of Kr, Xe and Hg Using Interacting Boson Models", Journal of University of Babylon for Pure and Applied Sciences, 28(1), 173-183, (2020).

[54] N. A. Sallal, "Low-Lying Spectra and (E2) Transition Rate in Even-Even $^{128-156}$Nd Isotopes Using IBM-1", M.Sc. thesis, University of Babylon, (2017).

[55] Gh. A. Jaber and M. K. Muttaleb, "Study the deformation in some even krypton isotopes (88-92) using IBM-1 model" In Journal of Physics: Conference Series, 1234(1), 012025, (2019).

[56] H. A. Marhoon , " Study of the energy levels for even-even $^{98-104}$Mo by using IBM-1", M.Sc. Thesis, Babylon University, (2010).

[57] P. Van Isacker, "Dynamical symmetries in the structure of nuclei", Reports on Progress in Physics, *62*(12), 1661–1717, (1999).

[58] F. Iachello and A. Arima, "Boson Symmetries in Vibrational Nuclei", Physics Letters, 53(4), 309–312, (1974).

[59] K. Nomura "Interacting boson model from energy density functionals", Ph.D. Theses, University of Tokyo, (2013).

[60] L. Frankfurt and M. Strikman, "Hard nuclear processes and microscopic nuclear structure", Physics Reports, 160(5-6), 235-427, (1988).

[61] Gh. A. Jaber and M. K. Muttale, "Effect The change in bosons on The properties of xenon isotopes", Arts, Humanities and Natural Sciences Conferences, (2019).

[62] P. Cejnar and J. Jolie, "Quantum phase transitions in the interacting boson model ", Progress in Particle and Nuclear Physics, 62(1), 210-256, (2009).

[63] K. S. Krane, "E2, M1 multipole mixing ratios in odd-mass nuclei, 59≤ A≤ 149", Atomic Data and Nuclear Data Tables, 19(4), 363-416, (1977).

[64] O. Scholten, "The interacting boson approximation model and applications", Ph.D. thesis, University of Groningen, (1980).

[65] M. K. Mohammed, "A study of nuclear structure of $^{130\text{-}150}$Ce even-even isotopes by the interacting boson model-1" ,thesis, University of Babylon, (2015).

[66] J. P. Elliott, "The interacting boson model of nuclear structure", Reports on Progress in Physics, 48, 171-221, (1985).

[67] O. Castanos , E. Chacón , A. Frank and M. Moshinsky, "Group theory of the interacting boson model of the nucleus", Journal of Mathematical Physics, 20(1), 35-44, (1979).

[68] A. Leviatan, "Partial dynamical symmetries", Progress in Particle and Nuclear Physics, 66(1), 93-143, (2011).

[69] J. Engel and F. Iachello, "Interacting boson model of collective octupole states (I). The Rotational Limit ", Nuclear Physics A, 472(1), 61–84, (1987).

[70] A. Arima and F. Iachello, "Interacting boson model of collective nuclear states II. the rotational limit", Annals of Physics, 111(1), 201-238, (1978).

[71] V. K. B. Kota and R. Sahu, "Structure of medium mass nuclei: deformed shell model and spin-isospin interacting boson model", CRC Press. (2016).

[72] D. D.Warner and R. F. Casten, "Interacting-boson-approximation E 2 operator in deformed nuclei" , Physical Review C, 25(4), (1982).

[73] A. Arima and F. Iachello," Interacting boson model of collective nuclear states IV. The O (6) limit", Annals of Physics, 123(2), 468-492, (1979).

[74] D. Bondatsos and E. David , "Interacting boson models of nuclear structure", Stanford , Pub. In the United State, By Oxford University Press, New York, (1988).

[75] D. D. Warner and R. F. Casten," Predictions of the interacting boson approximation in a consistent Q framework", Physical Review C, 28(4), 1798, (1983).

[76] A. A. Mehdi, "Investigation of nuclear structure for isotopes $^{114-132}$Te even-even using interacting boson model-1", M.Sc. Thesis, Babylon University, (2020).

[77]A. Y. Kazem, "A study of nuclear properties of $^{148-154}$Sm even-even isotopes by the interacting boson model-1 (IBM-1)", M.Sc. Thesis, Babylon University, (2010).

[78] P. Cejnar, J. Jolie and R. F. Casten," Quantum phase transitions in the shapes of atomic nuclei", Reviews of Modern Physics, 82(3), 2155, (2010).

[79] N. Turkan, "Search for E (5) behavior: IBM and Bohr – Mottelson model with davidson potential calculations of some even – even Xe isotopes", Nuclear and Particle Physics, 34(11), 2235–2247, 2007.

[80] D. Warner, "A triple point in nuclei", Nature, 420 (6916), 614-615, (2002).

[81] A. Y. Shaalan, "Study of the electromagnetic transition and mixing ratio for some even-even nuclie", M.Sc. Thesis, Babylon University, (2019).

[82] Y. D. Devi, and V. Kota, "sdg interacting boson model: hexadecupole degree of freedom in nuclear structure", Pramana, 39(5), 413-491, (1992).

[83] I. K. Jabir, "A study of nuclear properties of $^{112-130}$Xe even-even isotopes by the interacting boson model-1 (IBM-1)", M.Sc. Thesis , Babylon University, (2016).

[84] A. M. K. and T. M. Awwad, "A theoretical description of U(5) - SU(3) nuclear shape transitions in the interacting boson model", Progress in Physics, 1(5), 7–11, (2013).

[85] P. Christmas and P. Cross," Relative intensities of γ-rays from E_2 Transitions in the decay of ^{180m}Hf ", Nuclear Instruments and Methods, 174(3), 571-575, (1980).

[86] M. O. Waheed and F. I. Sharrad, "Determination of the $^{108-112}$Pd isotopes identity using interacting boson model", Nuclear Physics At Energy, 18(4), 313–318, (2017).

[87] K. A. Hussain, " Negative parity states and some electromagnetic transition properties of even-odd mercury isotopes", M.Sc. Thesis, Babylon University, (2015).

[88] F. H. Al-Khudair, A. R. Subber and A. F. Jaafer, "Shape transition and triaxial interaction effect in the structure of $^{152-166}$Dy isotopes", Communications in Theoretical Physics, 62(6), 847–858, (2014).

[89] Z. Podolyák, "Prolate-oblate shape transition in heavy neutron-rich nuclei", In Journal of Physics: Conference Series, 381(1), 012052, (2012).

[90] A. Subber, W. D. Hamilton, P. Park and K. Kumar, "An application of the dynamic deformation model to the tellurium isotopes", Journal of Physics G: Nuclear Physics, 13(2), pp. 161–175, (1987).

[91] P. Van Isacker, and J. Q. Chen, "Classical limit of the interacting boson Hamiltonian", Physical Review C, 24(2), 684, (1981).

[92] ENSDF, http:// www.nndc.bnl.gov/ensdf, (Nuclear data sheet), (2015).

[93] P. J. Brussaard and P. W. M. Glaudemans, "Shell-model applications in nuclear spectroscopy", North Holland Publishing Company, North Holland, (1977).

[94] T. Venkova and W. Andrejtscheff , "Transition strengths B (E2) in the yrast bands of doubly even nuclei. Atomic Data and Nuclear Data Tables", 26(2), 93-136, (1981).

الخلاصة

في هذا العمل تم دراسة التركيب النووي باستخدام نموذج البوزونات المتفاعل وبتطبيق برنامج IBM، الاصدار لسنة 1984 وبلغة الفورتران.

تم تخمين معاملات الهاملتوني لكل نوية وحسب التحديد الذي تعود اليه للحصول على افضل تطابق بين القيم النظرية والقيم العملية المتوفرة ولمستويات الطاقة المتهيجة الواطئة. كذلك تم حساب الانتقالات الكهربائية بين بعض المستويات المتهيجة ، عزم رباعي القطب الكهربائي و سطح طاقة الجهد للايزوتونات الزوجية- الزوجية ل(^{194}Po، ^{192}Pb ، ^{190}Hg، ^{188}Pt و ^{186}Os).

فضلا عن تحديد شكل النواة عن طريق دراسة طاقة جهد السطح باستخدام معادلات دالة هاملتوني للجهد والذي يعطي فكرة عن التشوه الذي يحدث في النواة من انحراف الخطوط الكنتورية وتجميعها في منطقة معينة.

تمت مقارنة النتائج مع البيانات العملية المتوفرة و قد لوحظ ان النتائج بتوافق جيد. وكما تم حساب نسب التفرع $(R, R'and\ R'')$. ان اهمية ذلك تكمن في تحديد موقع العناصر نسبة الى التحديدات الثلاثة SU(3) و O(6) و U(5)، و قد اشارت نتائج الدراسة الحالية ان العناصر المدروسة تقع ضمن مناطق انتقالية مختلفة، النتائج اظهرت ان العناصر ^{194}Po, ^{192}Pb تقع في المنطقة U(5)، العناصر ^{188}Pt ,^{190}Hg في المنطقة O(6)، والعنصر ^{186}Os في المنطقة الانتقالية O(6)- SU(3).

جمهورية العراق

وزارة التعليم العالي والبحث العلمي

جامعة بابل / كلية العلوم

قسم الفيزياء

دراسة خواص التركيب النووي لبعض الايزوتونات الزوجية-الزوجية باستخدام نموذج البوزونات المتفاعل الاول IBM-1

رسالة مقدمة الى

قسم الفيزياء /كلية العلوم /جامعة بابل

و هي جزء من متطلبات نيل درجة الماجستير في علوم الفيزياء

من قبل

زهراء عبد الامير كاظم كشاش

بكالوريوس في علوم الفيزياء (٢٠١٩)

باشراف

ا.د.

محمد عبد الامير كريم الشريفي

م.د.

غيداء عبد الحافظ جابر حسين

١٤٤٤هـ

٢٠٢٢ م